OPTIMIZATION OF METAL CUTTING PROCESS PARAMETERS WHILE MACHINING AISI-1045 STEEL

ARSALAN QASIM
(2010-NUST-MSE&M-N-14)

A THESIS SUBMITTED IN FULFILMENT OF THE REQUIREMENT FOR THE DEGREE OF MASTER IN SCIENCE

In

MANUFACTURING SYSTEMS ENGINEERING AND MANAGEMENT

INSTITUTE OF MANUFACTURING ENGINEERING
PAKISTAN NAVY ENGINEERING COLLEGE
NATIONAL UNIVERSITY OF SCIENCES AND TECHNOLOGY
KARACHI PAKISTAN

(AUG-2014)

DEDICATION

This work is dedicated to my family for their love, encouragement and endless patience throughout my studies. Their continuous prayers have helped me finish my thesis successfully.

Also, I dedicate this work to my teachers, who guided me at all stages of the study.

Name of Thesis Supervisor

Dr. Salman Nisar

Names of G.E.C. Members

Dr. Sajid Saleem

Dr. Aqueel Shah

Lt. Cdr. Akmal Ataullah

Name of External Examiner

Dr. Tahir Abdul Hussain Ratlamwala

DECLARATION

None of the material contained in this thesis has been submitted in support of any application for another degree or qualification of this or any other university or institution of learning.

ACKNOWLEDGEMENT

The author would like to thank Institute of Manufacturing Engineering at Pakistan Navy Engineering College, National University of Sciences and Technology for having made this research possible.

ABSTRACT

This research aims towards the optimization of cutting parameters for temperature and cutting forces, with defined limits of material removal rate, in orthogonal machining process of AISI 1045 steel work piece with different carbide cutting tools, by using Design of Experiment with Taguchi and Finite Element Method. The cutting parameters analyzed and optimized are Depth of Cut, Feed Rate, Cutting Speed and Rake Angle. These parameters are taken as factors in S/N ratio analysis and ANOVA. The use of optimized cutting parameters lead to enhanced tool life and reduced power consumption. For optimization of parameters Taguchi orthogonal array experiment design and Signal to Noise Ratio are utilized, and to save time and money the results of experiments are achieved through Finite Element Modeling using a general purpose FEM software ABAQUS®. The model created in FE software is verified by replicating experiments from literature and comparing the obtained results. It was found that carbide cutting tool is a better option while machining AISI 1045 steel as it results in lower cutting forces and temperature values as compared to uncoated cemented carbide cutting tool. The most significant factors found for cutting forces are feed rate and depth of cut while for temperature rake angle and cutting speed are found to be most significant factors.

Table of Contents

LIST OF FIGURES

LIST OF TABLES

NOMENCLATURE

T_r	Room Temperature
T_m	Melting Temperature
$\dot{\varepsilon}$	Strain Rate
v	Cutting speed
f	Feed rate
d	Depth of cut
$\dot{\varepsilon}_o$	Reference Strain Rate
τ_{cr}	Critical Friction Stress
μ	Coefficient of Friction
τ_f	Frictional Stress
F_c	Cutting Force
$\bar{\eta}_G$	Average S/N Ratio
F_{cal}	Statistically calculated Cutting Force using optimum parameters
T_{cal}	Statistically calculated Temperature using optimum parameters

ACRONYMS

AISI	American Iron and Steel Institute
ALE	Arbitrary Langrangian Eulerian
ANOVA	Analysis of Variance
CNC	Computer Numeric Control
DOE	Design Of Experiments
FEA	Finite Element Analysis
FEM	Finite Element Model
JC Model	Johnson Cook Model
MRR	Material Removal Rate
MSE	Mean Square Error
MSTR	Mean Square Treatment
S/N Ratio or SNR	Signal to Noise Ratio
SSE	Sum Square Error
SSTR	Sum Square Treatment

CHAPTER 1

INTRODUCTION

1.1 Background:

In today's modern industry manufacturers aim to manufacture high quality products in short time bearing the lowest cost possible. Automated and flexible manufacturing systems such as the computerized numerical control (CNC) machines are employed for that purpose, which are capable of minimizing the processing time while achieving high accuracy. Turning process is one of the most used methods for cutting and the finishing of machined parts. In this process, it is vital to select input (cutting) parameters with great precision for achieving high cutting performance. Generally, the required cutting parameters are chosen based on experience or by use of a handbook [1].

Research work has been done in optimizing the parameters like surface roughness, stress distributions in the workpiece, deformed chip shape etc through simulations and Design of Experiments. This research work is aimed to optimize the parameters for both temperature and cutting forces (having defined the limit for material removal rate) using Taguchi method with Finite Element Method. In addition to this, the research also includes multiple cutting tool materials for study which enhance the scope of this research instead of keeping it limited to a single tool.

The parameter optimization helps reduce the power consumption of cutting process and enhances tool life and hence will greatly influence the manufacturing cost.

American Iron and Steel Institute (AISI) 1045 Steel has been selected on purpose as the work piece material in this study as it is one of the most widely used grades of steel [2] It has a great application in the manufacturing processes due to its characteristics of low cost and high machinability [3]. It has also been used for research by various authors in the context of machining [4, 5]

Cutting parameters have to be selected carefully to be optimized for performance characteristics. For this four cutting parameters have been selected i.e. depth of cut, feed rate, rake angle and cutting speed. They were chosen as they are the basic independent parameters which are set by the operator and if these are optimized, they can have direct impact on the outputs. The performance characteristics to be improved are cutting forces and cutting temperatures.

1.2 Aims & Objectives:

Feasible ranges of each cutting parameter will be taken from handbook of machining and/or literature and each range will be divided into five levels. By the use of Taguchi Method the optimal level of each parameter will be determined. The Taguchi Method, an experimental design technique, is useful in minimizing the quanta of experiments effectively by the use of orthogonal arrays. This greatly reduces the time by identifying significant factors in lesser time.

Finite element codes have been used as an effective technique for analyzing material flow especially in the cutting process in particular. These methods are designed for problems which involve large elastic-plastic deformations with temperature dependent material properties and high strain rates [6].

The experiments will be conducted with Finite Element Modeling by using Arbitrary Lagrangian Eulerian (ALE) approach and the results will be fed to the Taguchi matrix.

Main objectives of this study are:

- Develop and validate a Finite Element Model (FEM) which can simulate the orthogonal cutting process with significant accuracy.
- Perform simulations using validated FE model by varying input parameters as per the selected Taguchi matrix
- Obtain optimum values for input via Signal-to-Noise Ratio and ANOVA which will result in lower values of cutting forces & temperature as output.
- Simulate the process using optimum input parameters to obtain statistically calculated optimum levels of cutting forces and temperatures.

CHAPTER 2

ORTHOGONAL MACHINING FUNDAMENTALS

2.1 Definition:

Metal cutting is a process in which shear deformation of work piece material is involved to form a chip. As the chip is formed, a new surface is exposed on the work piece.[7]

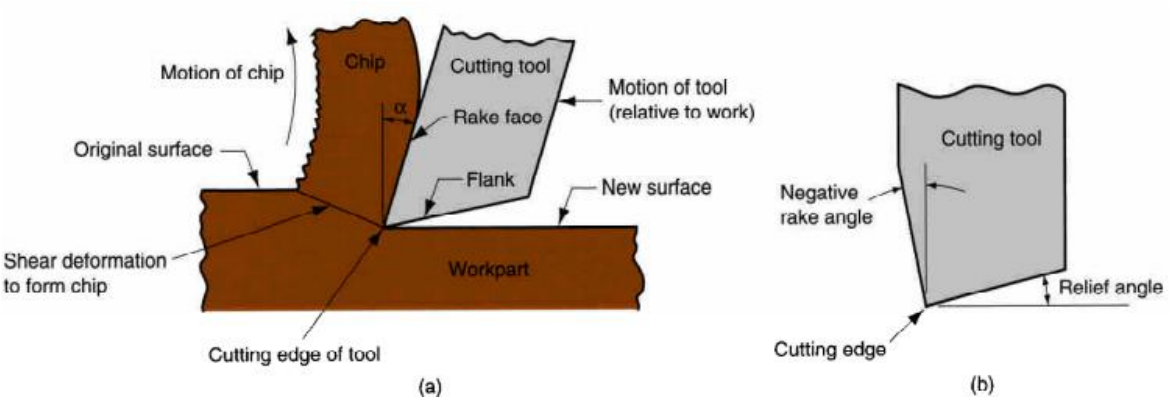

Figure 1 (a) Cross sectional view of the orthogonal cutting process (b) Tool with negative rake angle [7]

Orthogonal Cutting was first introduced by Merchant [8] who reported the concept of shear angle. Orthogonal cutting is a two dimensional simplified representation of the metal cutting process as shown in Figure 1(a) [7]. The motion of newly formed chip is almost perpendicular to the motion of the tool or work piece. This model has been studied and used by other authors in literature like E.H. Lee et. al. [9] and A.O. Tay et. al. [10]

2.2 Basic Advantages/ Disadvantages of Machining:

Machining process is used in a lot of applications and is often the most feasible option in the manufacturing universe. Some of its advantages include:

- Various materials can be machined into desirable forms.
- A lot of part shapes and geometry features are possible with machining like round holes on the surface of a plate or screw threads on a long bar.
- The process quality can be improved to near perfection with very little tolerance levels.

Some of it main disadvantages include:

- Material that is machined off is usually wasted in form of chips.
- Huge amount of heat is given off which contributes to energy waste
- Machining operations are generally time consuming as compared to other types of shape forming manufacturing processes like casting or powder metallurgy.

2.3 Cutting Conditions of Orthogonal Cutting Process:

The orthogonal cutting process involves a single point cutting tool which moves in the horizontal direction while the workpiece in contact with the tool revolves around the horizontal axis as shown in Figure 2 [7]. In a two dimensional representation, the process is shown in Figure 1(a).

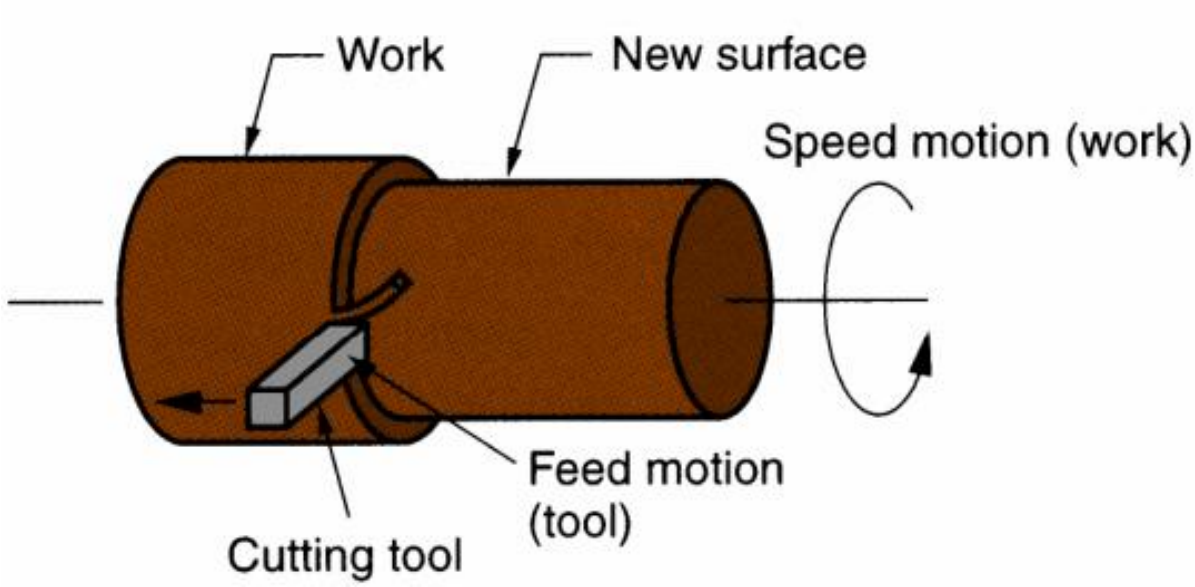

Figure 2 Simple turning process [7]

The following parameters are used in orthogonal machining process:

- Cutting Speed, which is the primary motion of tool with respect to work piece
- Feed, which is the length of work piece in contact with the tool, also knows as the undeformed chip length.
- Depth of Cut, which is the width of the cutting tool outside the two dimensional plane.

The material removal rate can be defined by Eq. 2.1

$$MRR = \ v * f * d \qquad \textbf{Eq. 2.1}$$

Where MRR is the material removal rate, “v” is cutting speed, “f” is feed rate and “d” is depth of cut as shown in Figure 3 [7].

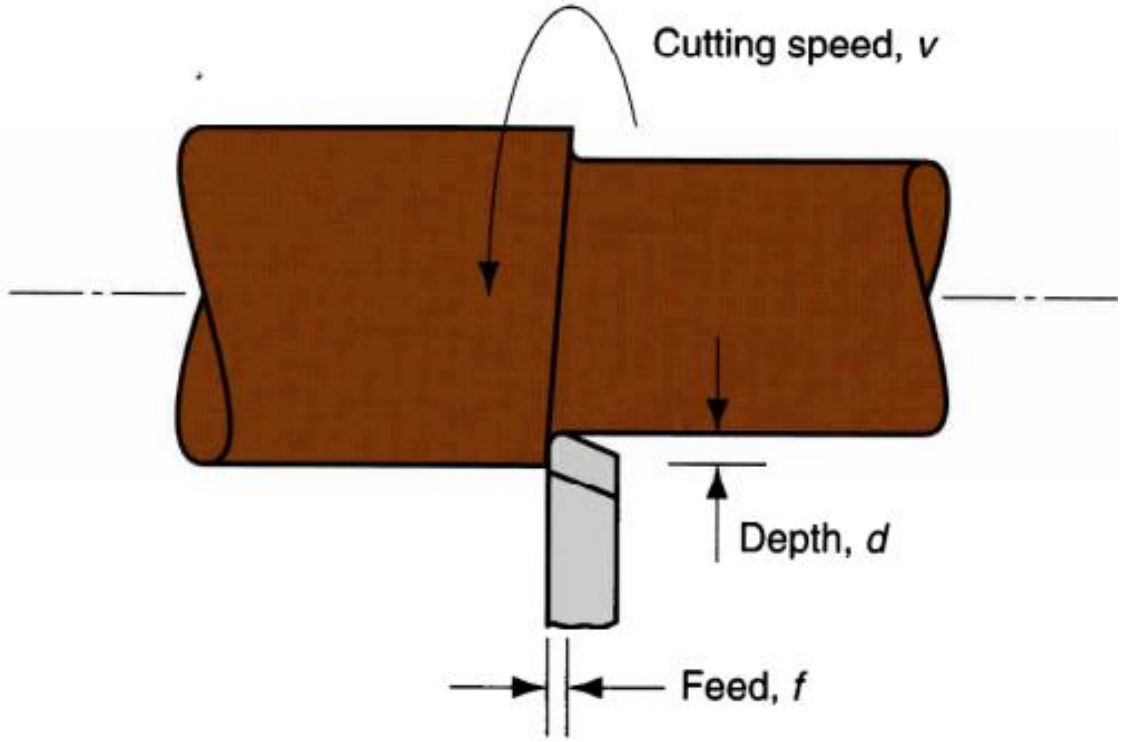

Figure 3 Cutting speed, Feed and Depth of Cut in Orthogonal cutting process [7]

CHAPTER 3

LITERATURE REVIEW

Many of the previous studies are based solely on experimental procedures and results having very little involvement of finite element analysis either analytical or simulation. [11,12,13]. The metal cutting process has been reported to reach high temperatures even upto 1000^{o}C [14,15]. Initially, very simple models were proposed and used by authors like the shear angle approach by Merchant [8, 16], Piispanen [17] and Oxley [18]. Lee and Shaffer [19] and Kudo [20] based their models on slip line theory using the concept of rigid-perfectly plastic material behavior. Later, the effects of work hardening [21, 22], friction [23] and built-up edge [24] were also included in the models.

The use of finite element model for cutting process simulation and optimization of parameters has now become very common and is used by many authors in their studies [25, 26, 27, 28, 29, 30, 31, 34, 35, 36, 37, 38, 39, 40]. Faraz et al. [39] has studied the effect of portion of heat going into the cutting tool during the orthogonal cutting process of AISI 4140 steel using a FE model. They have validated their model based on the realistic temperature of tool chip interface. Once validated, they have performed various analyses and provided results including effects of heat partitioning on the tool chip interface.

Mang Sung Choi [32] uses purely analytical calculations to find out the shear angle relationships on the shear plane in orthogonal cutting. Linhu Tang et. al [33] uses FEM to simulate the machining of AISI D2 tool steel with CBN cutting tool using dry hard orthogonal cutting process. Although very little work has been done in this regard, they do not conduct any experiments instead use the data already available in literature to verify their model and obtain results. They have used ABAQUS®, which is a general purpose finite element simulation tool, for modeling the process. Element removal technique based on nodal stresses has been adopted for chip formation using updated Lagrange model. An iterative technique for finding the friction coefficient is used while isotropic friction coefficient has been sought out from literature. Although the results obtained do fluctuate in terms of deviation from experimental results by a mean of 8%, this model is still considered to be good. For verification of results, they have conducted experimental procedures on a small setup.

Xiamon Deng et. al. [34] studied the finite element analysis orthogonal metal cutting process and effects of rake angle and friction coefficient was monitored on the parameters for temperature, stress, strain, and strain rate fields. To account for the local temperature rise due to conversion of friction work and plastic work in heat, adiabatic conditions are assumed. FE model was made using chip separation criterion and coulomb friction law was implemented for modeling dry friction between tool and chip. The simulations were run and contours for the 4 mentioned parameters were generated by varying rake angle and coefficient of friction.

M. Movahhedy et. al. [35] has used ALE formulation which can be considered as an upgraded Lagrangian or Eulerian formulation. It is reported that use of ALE gives better mesh adaptability but at the cost of a more complex model. However, remeshing techniques and chip separation criterions are avoided due to material flow around the tool.

Xiamon Deng et. al. [36] simulated the orthogonal cutting process of metal and noted the effects of friction on thermo mechanical quantities under plane strain conditions. He used modified coulomb's friction law in order to successfully model the phenomena of friction along the interface between tool and chip surfaces. To simulate the chip separation, finite element nodal release procedure was adopted. Rake angle and friction coefficients were varied and it was shown that the material near the tip of the tool experiences highest amount of plastic strain rate whereas shear straining was observed in the primary shear zone. Due to lack of experimental data, the values for failure stresses of the material were

assumed keeping in view the yield strength of the material used. Friction modeling is as per coulomb friction law in sticking and sliding region. Work piece is taken to be 10 mm in thickness. Tilted geometry is used to account for extreme distortion during chip formation. 16 simulations were carried out using variation of rake angle and coefficient of friction while noting their effects on temperature and cutting forces. To attain a steady state, the sticking region is monitored and steady state is considered when contact length remains constant.

Sutherland et. al. [37] developed a model involving thermo mechanical finite elements and used it for simulating orthogonal metal cutting process, with particular emphasis on the effect of crater wear considering plain strain & steady state conditions. Critical stress criterion is used for chip separation and general purpose finite element code ABAQUS® is used. Crater wear is identified as a geometric property of the crater formed on the tool rake face. This property is varied and simulations are run to study the effect of crater wear on the process. Size of the crater is reported here to have a great influence on the output of the simulation like curling radius. The results were presented on the basis of computational observations only and no physical tests were performed for cross checking the obtained results.

C. Shet and X. Deng [38] used FEM to simulate orthogonal metal cutting process focusing on the residual stress and strain fields in the finished work piece. The chip separation criteria used by them involved separation of joined nodes just ahead of the tip at a specific distance. Modified coulomb law, an option given in ABAQUS® is used to model friction between the tool and work piece. For energy dissipation modeling, it is assumed that 90% of the plastic work done is converted into heat energy. Furthermore, it is assumed that 50% of the total heat generated goes into the tool & 50% into the chip. Viscoelastic constitutive model of the over-stress power law type along with temperature dependent material properties are used to model the flow stress of the work piece. Simulation is done in four stages where the loads are applied then removed and work piece is then allowed to cool off. Results for residual stresses and strains in the finished work piece are reported using various coefficients of friction and rake angles.

Faraz et al. [39] used FEA code to simulate orthogonal machining of AISI 4140 steel with cemented carbide tool. They used thermal imaging to find out the amount of heat going into the tool and work piece and to measure temperature during machining. Because the elastic modulus of the tool material is very large as compared to that of the work piece material, the tool is assumed to be perfectly rigid. As done in previous studies, it is assumed that plane strain conditions exist. Chip separation criteria are defined along a pre defined chip formation path. To maintain the simulation time under practical limits, only a few milliseconds of simulation is performed. Johnson cook model is used as in many previous studies and is accepted as a highly successful model in high speed machining. Flow stress and damage constants are taken from previous studies. Coulomb's friction law is used to model sticking and sliding region on the tool-chip interface. The model is verified on the basis of cutting forces predicted from simulation being equal to the ones measured practically using a dynamometer. Once the model is verified, several parameters are reported and analyzed in the paper.

M. Mohammadpour et. al. [40] used a nonlinear finite element code MSC to develop a finite element analysis for investigating the effect of cutting speed and feed rate of surface and subsurface residual stresses. They did not use any chip separation criteria instead used adaptive remeshing techniques to model chip formation. Remeshing criteria are defined based on geometric properties of each element, distance between connecting body edges and frequency based. As done in previous studies, Johnson Cook model has been used for material flow stress modeling. A modified Oxley's model is implemented for friction modeling with JC flow stress model integrated into itself. Model is verified by comparing residual stress profiles with experimental data in literature. Simulations are carried out and results for temperature and stresses are reported at different cutting speeds.

Komvopoulos and Erpenbeck [41] studied the effects of plastic flow properties, tool-workpiece interface friction and wear on tool on the chip formation in orthogonal metal cutting process. the

simulation was achieved using “distance tolerance” criterion. Tyan and Yang [42] used the limit analysis theorem to analyze orthogonal metal cutting process. They used an Eulerian reference coordinate system in order to explain the steady state motion of workpiece relative to the tool.

CHAPTER 4

RESEARCH METHODOLOGY

4.1 FEA Model and Its Validation:

Simulation model for Finite Element Analysis (FEA) is created in a general purpose Finite Element Modeling (FEM) software ABAQUS® v6.10. This model is verified against experimental and calculated results in the literature. Once validated, this model is used to simulate orthogonal machining of AISI 1045 steel work piece and multiple tools as specified above. Machining tool, work piece & machining conditions (dynamic and static model boundary conditions) during validation are taken from the literature which the model is compared to.

4.2 Design of Experiments:

Since the number of tools, machining parameters and their levels all make up numerous combinations which are time consuming to simulate; Design of Experiments & Taguchi method are used to get a matrix of selected combinations on which to carry out the simulations.

4.3 Simulation:

Machining conditions for simulation using AISI 1045 work piece are varied to get the optimum value of conditions for each tool material and the various values are taken from literature.

4.4 Analysis:

Once the simulations are done and the results are in matrix form, Signal to Noise Ratio and ANOVA are used for each tool to obtain the best possible conditions for machining with that tool. Observations, results and conclusions are then compiled with the help of these analyses.

CHAPTER 5

FINITE ELEMENT ANALYSIS

5.1 Assumptions:

To simplify the process of modeling, simulation and its analysis, some assumptions need to be taken.

- The plane strain state is assumed, which is justifiable due to the fact that the cutting width is much larger than the undeformed chip thickness.
- The tool is taken to be perfectly elastic. This is justified as the elastic modulus of our tool is very large as compared to that of the work piece and therefore the small elastic deformations in the tool are negligible against the high plastic deformations of the work piece.
- To keep the simulations as simplified as possible, it is also assumed that the tool edge is perfectly sharp.

5.2 Geometrical Model:

The geometric model is made as a simple two dimensional representation of orthogonal cutting as done by many authors previously [11, 34, 37, 39]. The work piece is kept fixed while tool will move inwards to perform cutting operation thereby separating the chip from the work piece. Numerical simulations of the machining process were done by a specialized computational procedure made for a general purpose finite element code named ABAQUS®. The operating assembly diagram is given in Figure 4. Work piece dimensions are taken as 0.4 mm height and 2 mm length. Tool has a clearance angle of 7 degrees while rake angle is initially kept at 0 degrees. These specifications are used for validation of model and compared with the results of the model made by Faraz et. al.[39]. Later in the study, these will be changed according to experimental requirements.

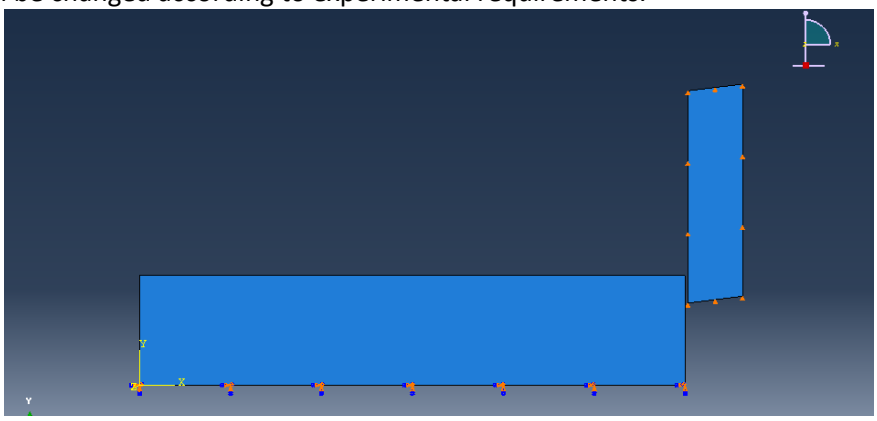

Figure 4 Geometric Assembly

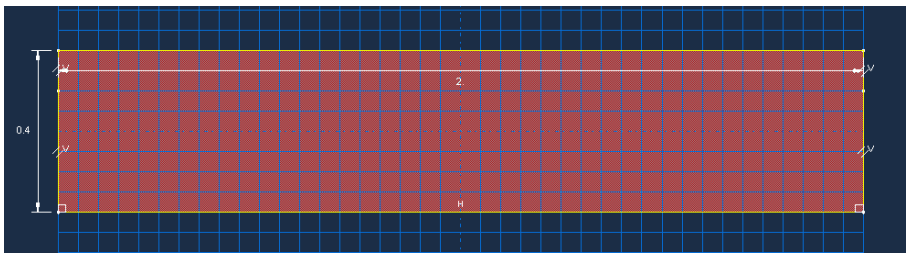

Figure 5 Dimensions of work piece

5.3 Johnson Cook Model:

Material flow behavior in the plastic regime may be constituted by many different constitutive models. To describe material flow behavior in the plastic regime over large strains, at high strain rates and at high temperatures [43] is described effectively by the Johnson-Cook (JC) material model [44]. This model considers the flow stress to be a product of three terms representing the effect of strain, strain rate and temperature [3]. Plastic properties of a material using JC Constants is defined by the Eq. 5.1 [44]

$$\sigma = [A + B\varepsilon^{n}]\left[1 + C\ln\left(\frac{\dot{\varepsilon}}{\dot{\varepsilon}_{o}}\right)\right]\left[1 - \left(\frac{T - T_{r}}{T_{m} - T_{r}}\right)^{m}\right] \quad \text{Eq. 5.1}$$

JC constants A, B, C, m & n are the five empirical constants that define the material plastic properties. These can be found by various tests and also exist quite abundantly in the literature. The JC constants for AISI 1045 steel are given in Table 1 [3].

Table 1 Johnson cook constants for AISI 1045 steel [3]

A	B	C	n	M
680.5502	655.9590	0.008626	0.13642	1.095500

5.4 Step Time:

Since machining process at high speeds is not easy to simulate accurately [39], simulations rarely reach steady states (where changes to output per unit time is minimal) and to keep processing times within practical limits, the simulation is run for only a few milliseconds of machining.

5.5 Boundary Conditions:

The tool is constrained to move in the horizontal direction only giving it the specified velocity as a velocity boundary condition. Work piece bottom edge is kept fixed and is given the sufficient degrees of freedom to move as appropriate for simulation. Gravity load is applied to the whole region of simulation. A graphical representation of boundary conditions used in the model are given in Figure 6

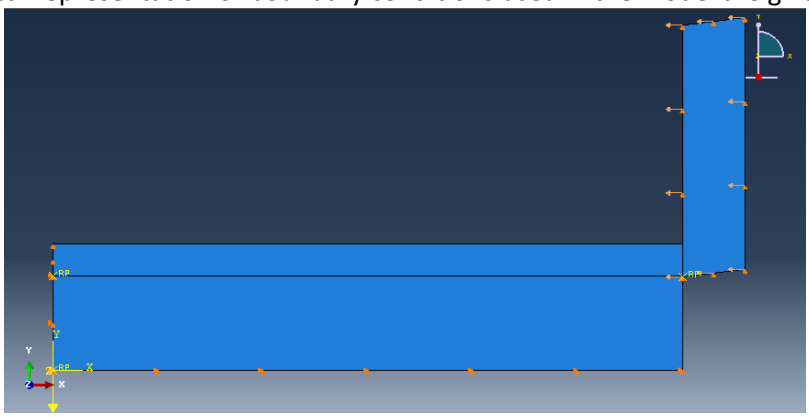

Figure 6 Boundary conditions used in the model

5.6 Friction Modeling:

One of the main aspects of metal cutting is the phenomenon of Friction. Along with determining the power required in removing the specified part of material it also keeps the quality of surface of the finished product in control as well as the rate at which the cutting tool wears off. To accurately model friction is a difficult task in metal cutting. Basically, as widely accepted, there are two individual contact regions, called the sliding and the sticking region which exist at the same time along the tool–chip interface. In the sliding region, a coefficient of friction referred to as μ exists which is often assumed with regard to the Coulomb friction law. Also, in the sticking region, a critical friction stress τ_{cr} is known to exist. [36]

The friction formulation type "penalty" is used which means that surface to surface interaction will be closer to physical phenomena as compared with "kinematic" type friction. A coefficient of friction of 0.3 is assumed for the contact interactions which is similar to the values assumed in many literatures [25, 36, 45]

The interaction between the newly formed chip and the tool used for cutting is deemed as a complex contact problem due to the fact that it involves elastic as well as plastic sheer stress and heat conduction along the tool and workpiece surfaces. Experimental observations in the literature report the existence of two distinct regions called the sticking and sliding regions, on the rake face of the tool used in the cutting process [4, 39]. In order to model the interface between tool and chip surfaces, Coulomb's friction law was used which is defined by the equations given in Eq. 5.2 [37]

$$\begin{aligned} \tau_f &= \mu p \qquad when \;\; \mu p < \tau_{max} \\ \tau_f &= \tau_{max} \qquad when \;\; \mu p \geq \tau_{max} \end{aligned} \qquad \textbf{Eq. 5.2}$$

The formulation involves friction coefficient (μ), equivalent shear stress (τ_{max}) and the frictional stress (τ_f) along the interface between tool and chip. The friction module which is readily available in general purpose code ABAQUS® was used as the friction model similar to its usage in many previous studies [37, 39, 46, 47].

5.7 Tool and Work Piece Material:

Work piece material AISI 1045 is used as specified in the previous chapter; its physical properties are given in Table 2 [3]. This work piece material will be used throughout the study except when the model is to be verified against experiments and simulations from literature.

Table 2 Material Properties of AISI 1045 steel [3]

Material Property	AISI 1045 Steel
Thermal Conductivity (k, W/m^{o}C)	48.3-0.023T
Young's Modulus (E, GPa)	210
Specific Heat (Cp, J/Kg^{o}C)	420+0.504T
Density (ρ, Kg/m^3)	7862
Thermal expansion coefficient (α, I^{o}C)	1.1 x 10^{-5}
Poisson Ratio (ν)	0.3

Since steel is used as workpiece in this study the most commonly used tools for steel are cemented carbides. Two different grades of cemented carbides have been chosen for current experimentation. The properties of both tools, as taken from literature are given in Table 3 [39, 48].

Table 3 Properties (Thermal/ Mechanical) of Cutting tools used [39, 48]

Parameter	carbide cutting tool material	uncoated cemented carbide cutting tool material
Poisson's Ratio	0.22	0.26
Specific Heat (J/Kg.K)	424	334
Young's Modulus (GPa)	534	630
Thermal Conductivity (W/m.K)	67.45	100
Density (Kg/m^3)	11900	11,900
Θ_{room} (room temperature, ^oC)	25	25

5.8 Type of Approach:

A pure Lagrangian approach means that the mesh moves with the material regardless of the deformation. The advantage of this approach is that the boundary is movable so there will always be the same number of elements in the material mesh. However, the drawback will be observed when there is excessive deformation and mesh grading is affected meaning difference in mesh density across the deformed area. This can lead to excessive distortions.

Unlike the Lagrangian approach, there is Eulerian approach where the boundaries are fixed i.e. mesh grid is fixed and the material moves in and out of the mesh. Here there is virtually no mesh degradation but it is difficult to model controlled mass experiments. This type of approach is ideal for situations where material flow occurs across the mesh boundary e.g. flow of fuel through the combustion chamber.

In problems where large deformation is anticipated the improved mesh quality resulting from adaptive meshing can prevent the analysis from terminating as a result of severe mesh distortion. In these situations one can use adaptive meshing to obtain faster, more accurate and more robust solutions than with pure Lagrangian analyses. [49]

The adaptive meshing technique in ABAQUS® combines the features of pure Lagrangian analysis and pure Eulerian analysis. This type of adaptive meshing is often referred to as Arbitrary Lagrangian-Eulerian (ALE) analysis. To maintain a high quality mesh throughout an analysis, ALE adaptive meshing is a handy tool, even when large deformation or loss of material occurs. It allows the mesh to move independently of the material. One of its limitations is that it does not alter the topology (connectivity and elements) of the mesh, which implies that it is difficult to maintain a high-quality mesh upon extreme deformation with this method.

5.8.1 Features of ALE Adaptive Meshing:

ALE adaptive meshing:

- Does not create or destroy elements, it maintains a topologically similar mesh throughout the analysis.
- Allows the mesh to move independently of the underlying material which helps maintain a high-quality mesh under severe material deformation

In ABAQUS®/Explicit ALE adaptive meshing:

- Can be used to analyze Lagrangian problems (in which no material leaves the mesh) and Eulerian problems (in which material flows through the mesh);
- Can be used as a continuous adaptive meshing tool for problems such as dynamic impact, penetration, forging problems or other transient analysis problems undergoing large deformations;

- Can be used as a solution technique to model steady-state processes like extrusion or rolling;
- Can be used as a tool to analyze the transient phase in a steady-state process [49]

ALE methodology is used in this study to obtain the desired results. It is found to be the best fit for the scope of this thesis as compared to the other two i.e. Lagrangian & Eulerian.

5.9 Validation of Model:

Since performing, analyzing & evaluating physical machining process is lengthy, time consuming, costly and complex in terms of accuracy, these constraints are avoided by the use of FE Simulations for this study. To ensure that the results are accurate, the experimental research work found in literature is replicated and once the results are verified by those reported in literatures, the model is used for further simulations.

For this purpose, literatures based on experimental as well as simulation data are required, like those found in the work of O. Pantalé et al [45] and Faraz et. al. [39]. A detailed modeling of the metal cutting process is conducted by O. Pantalé using JC damage model for modeling the effects of damage on the workpiece 42CrMo4 steel. Since the mechanics and working are similar to the current model, the results obtained and published by him are replicated by current model in order to validate it.

A comparison of the results of cutting forces obtained via various sources as reported by O. Pantalé along with results from our model are given in Figure 7 and Figure 8:

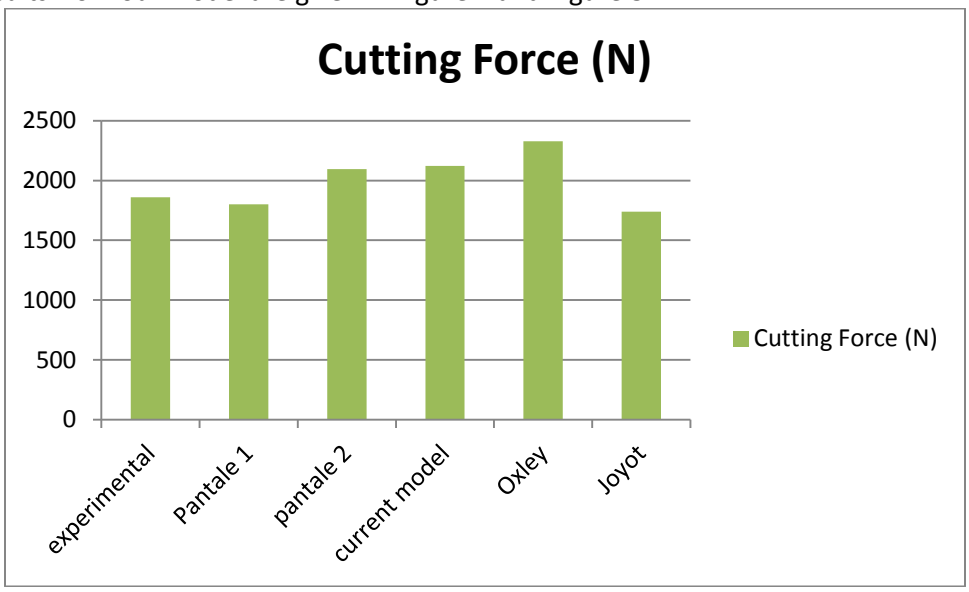

Figure 7 Cutting forces obtained by current model with results for cutting Forces published by O. Pantalé [45]

Source	Cutting Force (N)	% difference
experimental	1860	
Pantale 1	1800	-3.23%
pantale 2	2096	12.69%
current model	2121.571	14.06%
Oxley	2328	25.16%
Joyot	1740	-6.45%

Figure 8 Percentage Difference of Results of Current model vs Results reported by O. Pantalé et. al. [45]

Although it is not exactly as reported via experimental results, it is falling satisfactorily within the ranges reported by O. Pantalé. Since he did not publish any results related to temperature, the study by Faraz et. al. [39] was used for validation of temperature results.

Faraz et. al. [39] has studied the effect of portion of heat going into the cutting tool during the orthogonal cutting process of AISI 4140 steel. He has performed various analyses and provided results which can be used as a benchmark to validate the current model. The comparison between temperatures reported by Faraz et. al. [39] and the temperature values at different speeds by current model are given in Figure 9. The maximum difference between measured temperatures (using physical experimentation) and temperatures predicted by the current model is 2.5%

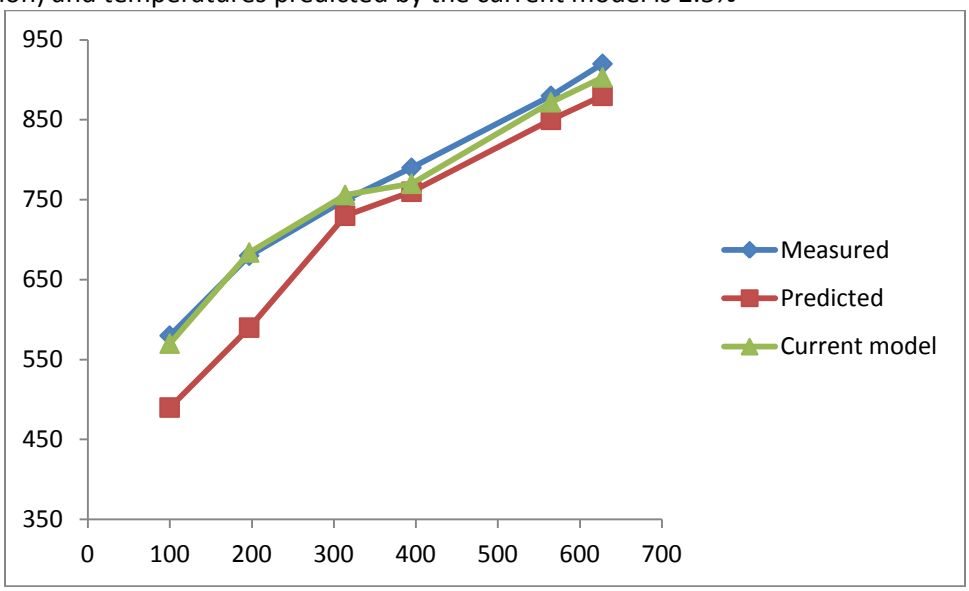

Figure 9 Comparison of Temperature values between model by Faraz et. al. [39] and Current model

Since both parameters i.e. cutting forces and temperatures are validated by literature data, experimentation can be done using this model.

CHAPTER 6

DESIGN OF EXPERIMENTS, SIMULATIONS & ANALYSIS

6.1 Introduction to Taguchi Method:

6.1.1 Background:

R.A.Fisher [50] first proposed the method of defining the conditions for experiments which involved more than one factors. It is commonly called the factorial design of experiments. For a given set of factors, all possible combinations will be identified by a full factorial design. Therefore, in most industrial experiments where a full factorial design is incorporated, a large number of experiments need to be done because of the significant number of factors involved. A more simplistic solution is to choose a small group of possible factors from all the possibilities in order to reduce the number of experiments. This method of choosing a minimal number of experimental runs while producing a huge amount of information is known as a partial fraction experiment. Taguchi's work is valuable as it gave us the general design guidelines which are important for factorial experiments and cover multiple applications such as quantitative researches done in the field of science and medicine where multiple treatments and subjects are involved.

6.1.2 Fundamental concepts:

Definition

Taguchi method is a unique method for designing the experiments. It is based on a set of well defined guidelines. Orthogonal arrays which are a kind of special set of arrays are used in this method [51]. These arrays define the method of minimizing the quantum of experiments down to a bare minimum which could still provide the complete data of all the factors affecting the parameters. The key to this method is selecting the level of combinations of the input variables or design variables for each experimental run.

A standard orthogonal array

Multiple standard orthogonal arrays exist which are used in the Taguchi method. Each of these arrays is used for a definite number of levels and independent input variables. Supposedly if an experiment is to be performed involving 4 distinct variables and each independent variable having 3 level values, then according to the array selector given by Stephanie Fraley et. al. [57], the L9 orthogonal array is used. It is generally assumed that interaction between factors does not exist. In many cases, this assumption is true; however, in actual practice interaction is obvious sometimes. In current study, the four factors selected are independent of each other.

Table 4 An Example of the L9 orthogonal array

The L_9 (3^4) Orthogonal array					
	Independent Factors				Performance Parameter Value
Run	Factor 1	Factor 2	Factor 3	Factor 4	
1	A	A	A	A	p1
2	A	B	B	B	p2
3	A	C	C	C	p3
4	B	A	B	C	p4
5	B	B	C	A	p5
6	B	C	A	B	p6
7	C	A	C	B	p7
8	C	B	A	C	p8
9	C	C	B	A	p9

An L_9 orthogonal array is shown in Table 4. There are a total of 9 experimental runs with each run based on a set of levels as given in the table. As an example, the ninth experiment involves the independent design variable 1 and variable 2 at level C, variable 3 at level B and variable 4 at level A.

Properties of an orthogonal array

The following special properties allow the orthogonal arrays to minimize the quantum of experimental runs required for the experiment.

Orthogonal arrays have a balancing property which means they consist of a special combination of levels and factors for each experiment designed such that all the levels in the vertical column under each independent factor appear an equal number of times. For e.g., in the L9 array in Table 4, under variable 4, level A, level B and level C appear thrice. It is mandatory that all the values of each level of independent variables be used for the experimental runs.

6.1.3 Assumptions of the Taguchi method:

The additive assumption of Taguchi method includes that the individual effects of the each independent variable (or their main effects) are separable on some or all performance parameters. Due to this assumption, it is possible for each factor to have an effect of any order i.e. linear order, quadratic or higher order. Also, it is assumed that no cross product effects (otherwise known as interactions) exist within the factors. In other words, the special level combinations of an independent variable do not cause any independent variable to have an effect on the performance parameters and vice versa. In case of violation of this assumption, the additivity of the main effects is eliminated causing interaction between the variables.

6.1.4 Experimental Design for Simulations:

The following steps are involved in the design of an experiment:

1. Independent variables in the study are identified and chosen for experimentation.
2. A quantum of level combinations for each independent variable/factor is specified and the resulting orthogonal array is chosen.
3. Conducting the experiments
4. Analyzing the data
5. Inference

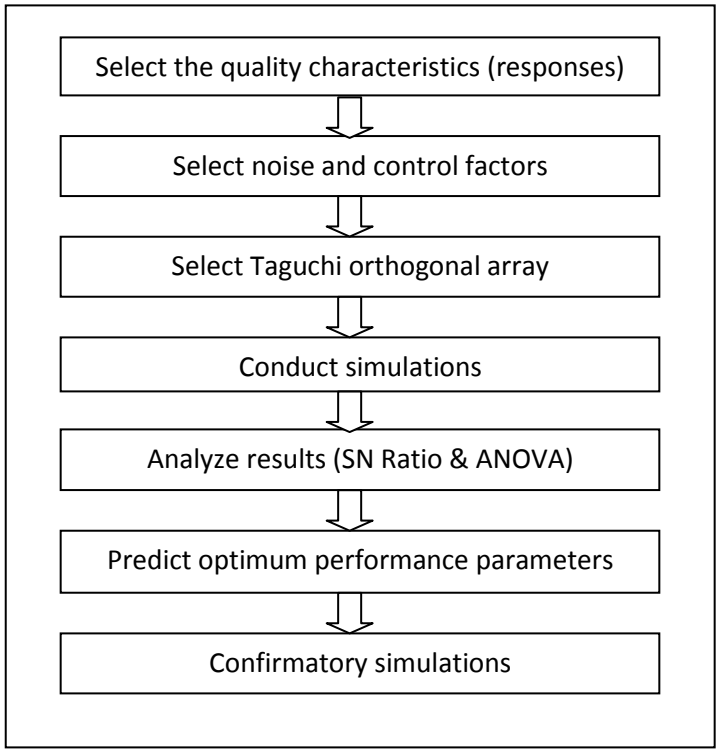

Figure 10 Steps of Taguchi Optimization process [54]

Following are the details of these steps.

Choosing the input (independent) variables

In order to identify the factors which are likely to influence the outcome of our experiment, knowing the product and process that is under investigation, is important before the experimentation begins. Selection of the independent variables is largely based on input from previous studies, people involved in the experiment, literary works etc. In the current study, cutting speed, rake angle, depth of cut and feed rate are chosen as the independent variables.

Deciding the number of levels and orthogonal array

This is the second step, after selecting the independent variables of the experiment, where the quantum of levels for every independent variable in the study is specified. This choice depends on how these distinct levels affect the parameters of performance. So, if it is a linear function, then the total level settings may be 2. But, in case the variable is not related linearly i.e. it is quadratic, cubic or of higher order, then one could go for higher levels.

In the case where exact nature of relationship between the performance parameter and the variable is unknown, two-level settings can be selected. Then, post the analysis of the data from experiments, a decision can be made based on the percent contribution and the error calculations if the assumption of level setting is right or not. Since the parameters chosen in the current study do not have any algebraic relationship with the process, five levels of each variable are set to ensure a wide spectrum and better results of optimization.

Conducting the experiment

When the selection of Taguchi orthogonal array for the experiment is done, the experimental runs are executed according to the level settings in the taguchi matrix. It is mandatory to conduct all the experiments as per the matrix. Although the dummy variable columns and interaction columns can be ignored while conducting the experimental runs, they are still required when the analysis of data is being done, in order to identify the effect of interactions.

6.1.5 S/N Ratio:

Signal to noise ratio, usually referred to as S/N Ratio, is one of the most effective and commonly used tool for evaluation of optimum design parameters. It is defined as the ratio of the desired signal to the random undesired noise. It gives the quality characteristics of data obtained from results of experiments. S/N Ratio has three functions which are chosen according to the criteria of optimum values for all factors. These functions are known as the objective function named as 'the-larger-the-better', 'the-smaller-the-better' and 'the-nominal-the-best'. In current study, both response variables Cutting force and Temperature are required to be as small as possible therefore "smaller is best" criteria is selected to calculate S/N Ratio as given in Eq. 6.1 [52]. The calculation is done using Minitab® v16.

$$SN\ Ratio = -10.\log\left(\frac{1}{n}.\sum_{i=1}^{n} Y_i^2\right)\ dB \qquad \textbf{Eq. 6.1}$$

Where n is the number of experiments and Y_i is the response of the i^{th} experiment. As stated previously, each experiment in the Taguchi matrix is a combination of different levels of factors. Therefore, it is important to isolate the distinct effect of all variables on the performance parameters. This is done by adding the S/N ratios of performance parameters for the respective level combinations.

Simply put, if one wishes to know the main effects of level A of the independent factor 2 (refer Table 4), one can find it by summing up the SN Ratios of performance parameter of the experiments 1, 4 and 7.

Several difficulties with the analysis of SN Ratios are cited in literature [52]. Some of these are as follows:

- Identification of active factors might not be reliable.
- In some cases, factors that do not have an impact on SN ratio, but affect the responses of experiments may exist.

As a secondary check on the analysis, ANOVA methods can be used for the responses which often provide a more detailed and informative assessment of active factors [52].

6.1.6 Analysis Of Variance (ANOVA):

ANOVA or "Analysis Of Variance" helps in the comparison of a number of population means, i.e. the means of a single factor for several populations. In one-way ANOVA, the variation among the sample means by a weighted average of their squared deviations about the mean is measured for all the sample data. That measure of variation is called the treatment mean square, MSTR, and is defined in Eq. 6.2

$$MSTR = \frac{SSTR}{k-1} \quad \textbf{Eq. 6.2}$$

Where "k" denotes the number of populations being sampled. SSTR, also known as treatment sum of squares, is given by the Eq. 6.3.

$$SSTR = n_1(\bar{x}_1 - \bar{x})^2 + n_2(\bar{x}_2 - \bar{x})^2 + \cdots + n_k(\bar{x}_k - \bar{x})^2 \quad \textbf{Eq. 6.3}$$

Next the measure of variation within the samples is considered. This measure is the pooled estimate of the common population variance, σ^2. It is called the error mean square, MSE, and is defined in Eq. 6.4 [53].

$$MSE = \frac{SSE}{n-k} \quad \textbf{Eq. 6.4}$$

Where "n" denotes the total number of observations. SSE or error sum of squares is given by

$$SSE = (n_1 - 1){s_1}^2 + (n_2 - 1){s_2}^2 + \ldots + (n_k - 1){s_k}^2$$

Where "s^2" is the variance of each population. Finally, the F-statistic (factor statistic) is used to compare the variation among the sample means, MSTR, to the variation within the samples, MSE. It is given by Eq. 6.5 [53]. Large values of F indicate that the variation among the sample means is large relative to the variation within the samples [53].

$$F = \frac{MSTR}{MSE} \quad \textbf{Eq. 6.5}$$

Using these identities a table is formed for one way ANOVA as given in Table 5.

Table 5 ANOVA Table

Source	DoF	SS	MS	F-stastic
Treatment	k – 1	SSTR	MSTR	F
Error	n – k	SSE	MSE	
Total	n - 1	SST		

6.1.7 Inference:

Once the SN response table and ANOVA table have been populated, they are used to determine the statistical significance and optimum combination of the experimental parameters. The SN response table will identify the factors which have the most impact on the outcome of the experiment and ANOVA will confirm the probability of these factors being within the limits. In other words, SN ratio gives a directional evidence of significant factors while ANOVA tests verify the statistical probability of those factors being most significant using F-statistic value.

The results are then confirmed by conducting confirmatory experiments when the optimum parameters, found by Taguchi optimization method, were used as input and thus the validity of the experimental results is tested.

6.2 SIMULATIONS:

6.2.1 Selection of Range and Parameter Levels:

Following table gives the levels of factors to be used in the simulation. The different values for each design variable are selected to cover a wide range of cutting conditions. These ranges are based on various DOE factor levels found in practices and literature [4] [25] [39] [54] [55]. Having excess width in the range of these parameters can also lead to poor response quality [56] and therefore may not produce the results that would help us determine the optimum conditions. That is the reason for not selecting any parameters on their extreme values for example, cutting speeds lower than 100 m/min or higher than 630 m/min are not common in the cutting of steels. Likewise, all parameters are chosen within moderate ranges as given in literatures and to ensure the range is well covered within five-levels, appropriate spacing is given between them.

Table 6 DOE Factors and Level values for Simulation with AISI 1045 Steel

Parameters	Level 1	Level 2	Level 3	Level 4	Level 5
Cutting Speed (m/min)	100	200	400	550	630
Feed Rate (mm)	0.05	0.07	0.1	0.15	0.2
Rake Angle	-2^{o}	0^{o}	3^{o}	5^{o}	7^{o}
Depth of Cut (mm)	1	1.5	2	2.5	3

Table 7 Response Variables for DOE

Response	Output
R_1	Cutting Force (N)
R_2	Temperature (^{o}C)

6.2.2 Selection of Orthogonal Array:

According to the array selector given by Stephanie Fraley et. al. [57], if there are 4 control variables and 5 levels of each in the DOE as specified in the previous section, the Taguchi $L_{25}(5^4)$ array is to be utilized. This array is tabulated in Table 8.

Table 8 Taguchi L_{25} Array with Variable Ranges from Current Study

Runs	Cutting Speed (m/min)	Feed Rate (mm)	Rake Angle	Depth Of Cut (mm)
1	100	0.05	-2	1.0
2	100	0.07	0	1.5
3	100	0.10	3	2.0
4	100	0.15	5	2.5
5	100	0.20	7	3.0
6	200	0.05	0	2.0
7	200	0.07	3	2.5
8	200	0.10	5	3.0
9	200	0.15	7	1.0
10	200	0.20	-2	1.5
11	400	0.05	3	3.0
12	400	0.07	5	1.0
13	400	0.10	7	1.5
14	400	0.15	-2	2.0
15	400	0.20	0	2.5
16	550	0.05	5	1.5
17	550	0.07	7	2.0
18	550	0.10	-2	2.5
19	550	0.15	0	3.0
20	550	0.20	3	1.0
21	630	0.05	7	2.5
22	630	0.07	-2	3.0
23	630	0.10	0	1.0
24	630	0.15	3	1.5
25	630	0.20	5	2.0

6.3 Results of Simulations:

After running all the above given combinations of factors with each cutting tool, the results obtained for response variables are given in Table 9 and Table 10.

Table 9 Responses of Simulations with Carbide Cutting tool (Source: ABAQUS®)

Runs	Cutting Speed (m/min)	Feed Rate (mm)	Rake Angle	Depth Of Cut (mm)	Cutting Force (N)	Temperature (^{o}C)
1	100	0.05	-2	1.0	143	525
2	100	0.07	0	1.5	252	534.5
3	100	0.10	3	2.0	451	539.2
4	100	0.15	5	2.5	674	518.2
5	100	0.20	7	3.0	873	515
6	200	0.05	0	2.0	276	668.4
7	200	0.07	3	2.5	430	688.8
8	200	0.10	5	3.0	652	698.6
9	200	0.15	7	1.0	281	715.2
10	200	0.20	-2	1.5	487	735.6
11	400	0.05	3	3.0	403	823
12	400	0.07	5	1.0	174	700
13	400	0.10	7	1.5	320	617.7
14	400	0.15	-2	2.0	422	809
15	400	0.20	0	2.5	801	808
16	550	0.05	5	1.5	203	673.5
17	550	0.07	7	2.0	361	613.2
18	550	0.10	-2	2.5	549	917.1
19	550	0.15	0	3.0	802	858.1
20	550	0.20	3	1.0	338	1001
21	630	0.05	7	2.5	323	625.5
22	630	0.07	-2	3.0	501	796.2
23	630	0.10	0	1.0	202	821
24	630	0.15	3	1.5	400	812.9
25	630	0.20	5	2.0	651	891.2

Table 10 Responses of Simulations with Uncoated Cemented Carbide Tool (Source: ABAQUS®)

Runs	Cutting Speed (m/min)	Feed Rate (mm)	Rake Angle	Depth Of Cut (mm)	Cutting Force (N)	Temperature (^{o}C)
1	100	0.05	-2	1.0	153	568.8
2	100	0.07	0	1.5	251	648.9
3	100	0.10	3	2.0	428	545.1
4	100	0.15	5	2.5	649	573.4
5	100	0.20	7	3.0	925	551.3
6	200	0.05	0	2.0	276	536.8
7	200	0.07	3	2.5	463	707.4
8	200	0.10	5	3.0	644	714.9
9	200	0.15	7	1.0	258	578.3
10	200	0.20	-2	1.5	473	693.1
11	400	0.05	3	3.0	426	648.1
12	400	0.07	5	1.0	172	752.7
13	400	0.10	7	1.5	320	621.1
14	400	0.15	-2	2.0	573	765.6
15	400	0.20	0	2.5	774	854.0
16	550	0.05	5	1.5	212	833.0
17	550	0.07	7	2.0	333	678.5
18	550	0.10	-2	2.5	523	863.7
19	550	0.15	0	3.0	813	861.5
20	550	0.20	3	1.0	335	729.3
21	630	0.05	7	2.5	327	653.1
22	630	0.07	-2	3.0	552	768.9
23	630	0.10	0	1.0	211	746.0
24	630	0.15	3	1.5	410	926.4
25	630	0.20	5	2.0	660	980.8

6.4 Analysis:

6.4.1 Signal to Noise Ratio:

SN ratios for Cutting forces and Temperatures for both tools are given in Table 11 and Table 12. The calculation is done using Minitab® v16.

Table 11 SN ratios for experiments using carbide cutting tool (Source: Minitab®)

Experiment	Cutting Speed (m/min)	Feed Rate (mm)	Rake Angle	Depth Of Cut (mm)	Cutting Force (N)	S/N Ratio for F_c	Temperature (^oC)	S/N Ratio for Temp
1	100	0.05	-2	1	143	-43.1067	525	-54.4032
2	100	0.07	0	1.5	252	-48.028	534.5	-54.559
3	100	0.1	3	2	451	-53.0835	539.2	-54.635
4	100	0.15	5	2.5	674	-56.5732	518.2	-54.2899
5	100	0.2	7	3	873	-58.8203	515	-54.2361
6	200	0.05	0	2	276	-48.8182	668.4	-56.5007
7	200	0.07	3	2.5	430	-52.6694	688.8	-56.7619
8	200	0.1	5	3	652	-56.285	698.6	-56.8846
9	200	0.15	7	1	281	-48.9741	715.2	-57.0886
10	200	0.2	-2	1.5	487	-53.7506	735.6	-57.3328
11	400	0.05	3	3	403	-52.1061	823	-58.308
12	400	0.07	5	1	174	-44.811	700	-56.902
13	400	0.1	7	1.5	320	-50.103	617.7	-55.8156
14	400	0.15	-2	2	422	-52.5062	809	-58.159
15	400	0.2	0	2.5	801	-58.0727	808	-58.1482
16	550	0.05	5	1.5	203	-46.1499	673.5	-56.5668
17	550	0.07	7	2	361	-51.1501	613.2	-55.752
18	550	0.1	-2	2.5	549	-54.7914	917.1	-59.2483
19	550	0.15	0	3	802	-58.0835	858.1	-58.6708
20	550	0.2	3	1	338	-50.5783	1001	-60.0087
21	630	0.05	7	2.5	323	-50.1841	625.5	-55.9245
22	630	0.07	-2	3	501	-53.9968	796.2	-58.0204
23	630	0.1	0	1	202	-46.107	821	-58.2869
24	630	0.15	3	1.5	400	-52.0412	812.9	-58.2007
25	630	0.2	5	2	651	-56.2716	891.2	-58.9995

Table 12 SN ratios for experiments using uncoated cemented carbide cutting tool (Source: Minitab®)

Experiment	Cutting Speed (m/min)	Feed Rate (mm)	Rake Angle	Depth Of Cut (mm)	Cutting Force (N)	S/N Ratio for F_c	Temperature (^oC)	S/N Ratio for Temp
1	100	0.05	-2	1	153	-43.6938	568.8	-55.0992
2	100	0.07	0	1.5	251	-47.9935	648.9	-56.2436
3	100	0.1	3	2	428	-52.6289	545.1	-54.7295
4	100	0.15	5	2.5	649	-56.2449	573.4	-55.1692
5	100	0.2	7	3	925	-59.3228	551.3	-54.8278
6	200	0.05	0	2	276	-48.8182	536.8	-54.5963
7	200	0.07	3	2.5	463	-53.3116	707.4	-56.9933
8	200	0.1	5	3	644	-56.1777	714.9	-57.0849
9	200	0.15	7	1	258	-48.2324	578.3	-55.2431
10	200	0.2	-2	1.5	473	-53.4972	693.1	-56.8159
11	400	0.05	3	3	426	-52.5882	648.1	-56.2328
12	400	0.07	5	1	172	-44.7106	752.7	-57.5324
13	400	0.1	7	1.5	320	-50.103	621.1	-55.8632
14	400	0.15	-2	2	573	-55.1631	765.6	-57.68
15	400	0.2	0	2.5	774	-57.7748	854	-58.6292
16	550	0.05	5	1.5	212	-46.5267	833	-58.4129
17	550	0.07	7	2	333	-50.4489	678.5	-56.631
18	550	0.1	-2	2.5	523	-54.37	863.7	-58.7273
19	550	0.15	0	3	813	-58.2018	861.5	-58.7051
20	550	0.2	3	1	335	-50.5009	729.3	-57.2581
21	630	0.05	7	2.5	327	-50.291	653.1	-56.2996
22	630	0.07	-2	3	552	-54.8388	768.9	-57.7174
23	630	0.1	0	1	211	-46.4856	746	-57.4548
24	630	0.15	3	1.5	410	-52.2557	926.4	-59.336
25	630	0.2	5	2	660	-56.3909	980.8	-59.8316

6.4.2 Response data for S/N Ratios:

Response table consists of four types of data: average SN Ratio or average SNR, delta, rank and optimum level. The average SNR of each level of each factor forms the body of the table. For e.g. the average SNR for F_c of cutting speed level 1 is -51.92 (refer Table 13) and so on for all other factors and levels. Delta is the difference between the highest and lowest average SNR among all levels of a particular factor. For e.g. the highest and lowest values in cutting speed average SNR are -51.52 and -52.15 (refer Table 13) and their difference is 0.63 which is Delta for cutting speed. Rank is given to each factor according to their Delta value arranged in ascending order. Since Depth of Cut has the highest Delta among all four factors, it is given Rank 1(refer Table 13). This shows which factor has the most effect on the outcome of the experiment. Optimum level is selected on the basis of highest SNR among all levels in a particular factor.

The main effects graphs plot the average SN ratios against all levels of each factor. It is a graphical representation of the response table. The projection of graph on vertical axis gives value for Delta by calculating the differences between extreme values. The highest point of graph indicates the optimum level. Theoretically, the higher this graph goes, the higher impact that particular level has on that parameter towards the criteria of SN Ratio calculation. For e.g. the optimum level for feed rate in Figure 11 is level 1 which means using that level for simulations will cause the lowest value of F_c since the criteria selected was “smaller is best”.

Response tables for both cutting tools are given in Table 13, Table 14, Table 15 and Table 16 while Main effects plot for S/N Ratios of both response parameters using both tools are given in Figure 11, Figure 12, Figure 13 and Figure 14.

Table 13 Response Table for F_c using SN data for Carbide cutting tool (Source: Minitab®)

Level	Cutting Speed	Feed Rate	Rake Angle	Depth Of Cut
1	-51.92	-48.07	-51.63	-46.72
2	-52.1	-50.13	-51.82	-50.01
3	-51.52	-52.07	-52.1	-52.37
4	-52.15	-53.64	-52.02	-54.46
5	-51.72	-55.5	-51.85	-55.86
Delta	0.63	7.43	0.47	9.14
Rank	3	2	4	1
Optimum level	3	1	1	1

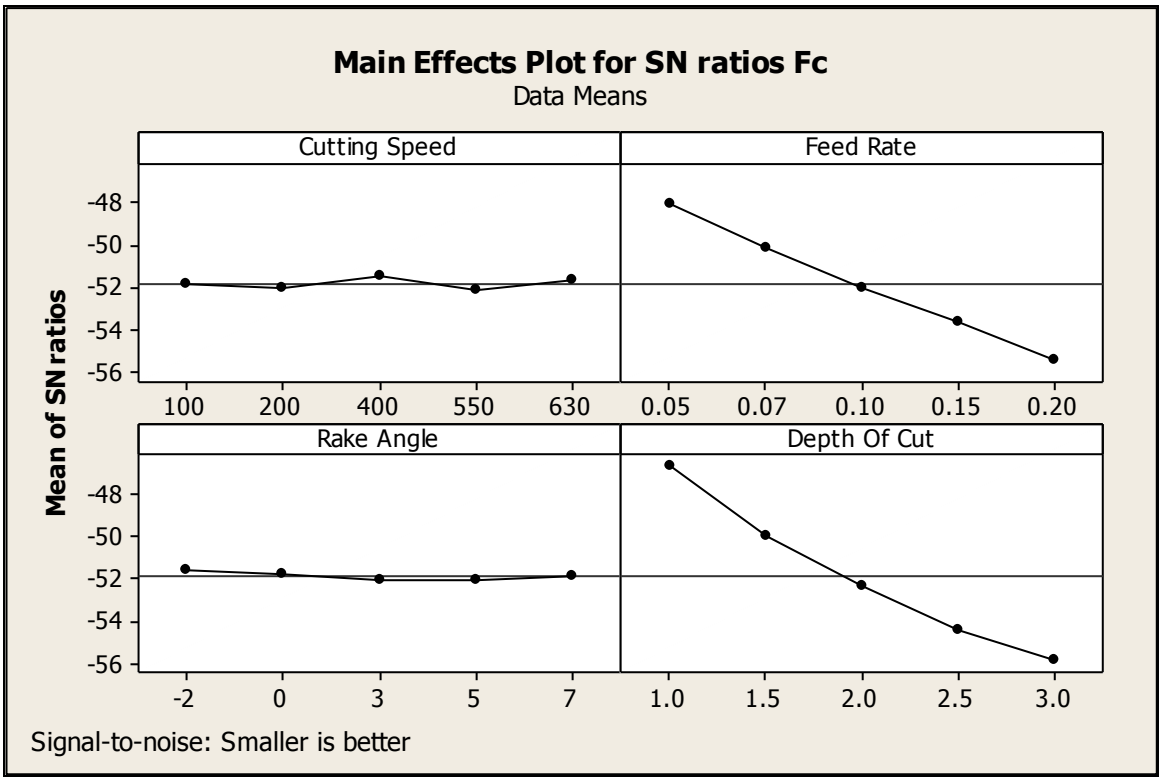

Figure 11 Plot for Main Effects for SN Ratios on F_c using Carbide Cutting Tool (Source: Minitab®)

Table 13 and Figure 11 shows that Feed Rate and Depth of Cut have the most variations in average SNR values hence this indicates these two factors are important to optimize if Cutting Forces are to be minimized. The optimum level for Feed Rate and Depth of Cut is found to be 0.05 mm and 1 mm respectively. As the graph shows, had there been any lower values of these two factors, they may be taken as optimum values, but as explained above, the range of these factors is decided based on literature and practical experiences so any value lower than these might not be commonly practiced.

Table 14 Response Table for Temp using SN data for Carbide cutting tool (Source: Minitab®)

Level	Cutting Speed	Feed Rate	Rake Angle	Depth Of Cut
1	-54.42	-56.34	-57.43	-57.34
2	-56.91	-56.4	-57.23	-56.49
3	-57.47	-56.97	-57.58	-56.81
4	-58.05	-57.28	-56.73	-56.87
5	-57.89	-57.75	-55.76	-57.22
Delta	3.62	1.4	1.82	0.84
Rank	1	3	2	4
Optimum level	1	1	5	2

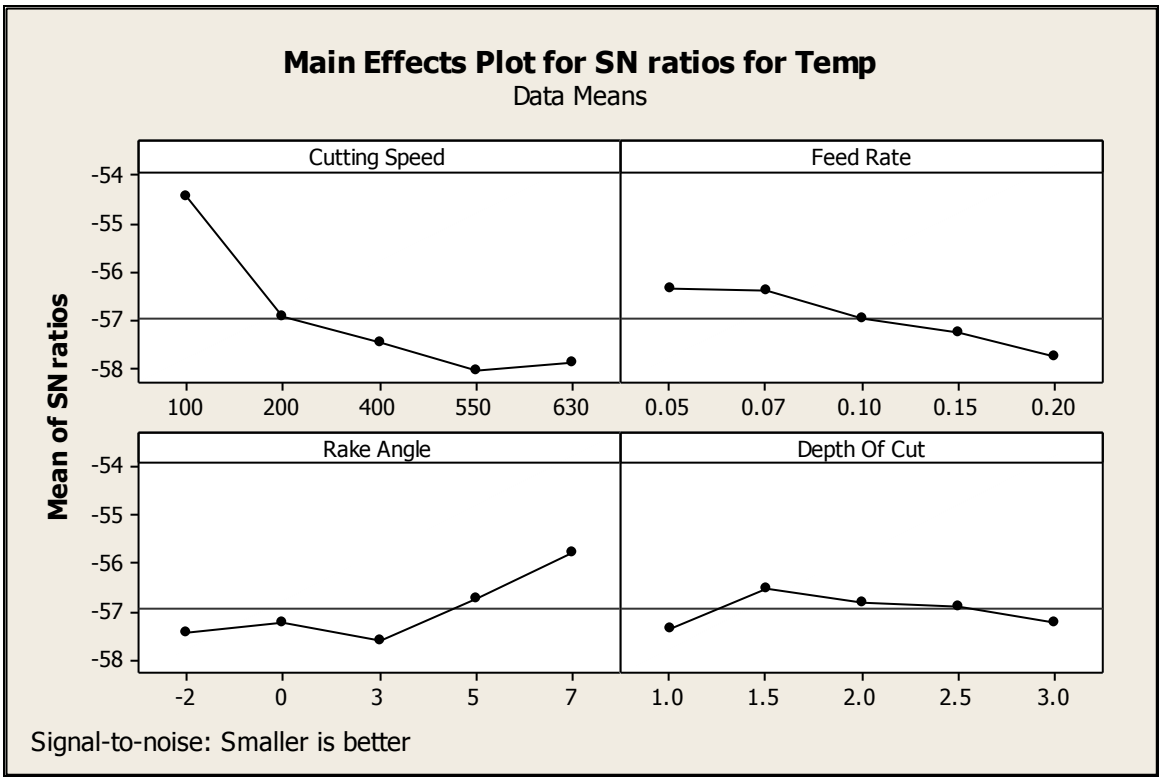

Figure 12 Plot for Main Effects for SN Ratios on Temp using Carbide Cutting Tool (Source: Minitab®)

Table 14 and Figure 12 represent the response data for SN values of Temperature for Carbide cutting tool. It is observed that for optimizing the temperature, the cutting speed has the most impact on outcomes followed by Rake Angle. The cutting speed directly affects friction and so lower cutting speed will logically have lower temperature values. Higher rake angle provides better slope for the deformed chip material to flow while lower rake angle (straight tool) would force the tool to move perpendicular to the motion. The optimum values for these two factors are found to be 100 m/min and 7^{o}. As explained above, these values are from the most widely used ranges so going beyond them would be difficult to implement widely.

Table 15 Response Table for F_c using SN data for Uncoated Cemented Carbide cutting tool (Source: Minitab®)

Level	Cutting Speed	Feed Rate	Rake Angle	Depth Of Cut
1	-51.98	-48.38	-52.31	-46.72
2	-52.01	-50.26	-51.85	-50.08
3	-52.07	-51.95	-52.26	-52.69
4	-52.01	-54.02	-52.01	-54.4
5	-52.05	-55.5	-51.68	-56.23
Delta	0.09	7.11	0.63	9.5
Rank	4	2	3	1
Optimum level	1	1	5	1

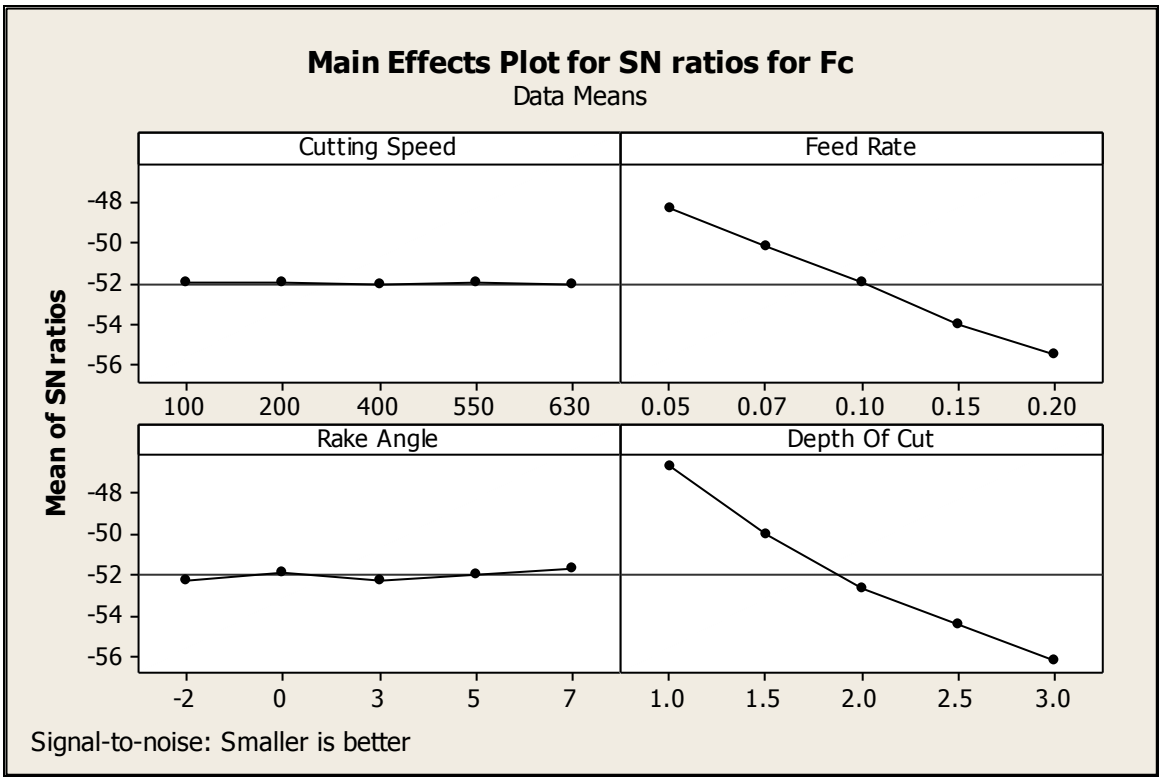

Figure 13 Plot for Main Effects for SN Ratios on F_c using Uncoated Cemented Carbide cutting tool (Source: Minitab®)

Table 15 and Figure 13 show the response data for SN values of cutting forces for uncoated cemented carbide cutting tool. Similar to the previous tool, these graphs also indicate the factors Feed Rate and Depth of Cut have the most impact on the outcome of the experiment. The optimum values found here are same as the previous tool i.e. 0.05mm Feed Rate and 1 mm Depth of Cut. It is logical to think that for minimum forces, one should keep the undeformed chip dimensions to a minimum and since these values are the least in the selected ranges, this outcome is logical.

Table 16 Response Table for Temp using SN data for Uncoated Cemented Carbide cutting tool (Source: Minitab®)

Level	Cutting Speed	Feed Rate	Rake Angle	Depth Of Cut
1	-55.21	-56.13	-57.21	-56.52
2	-56.15	-57.02	-57.13	-57.33
3	-57.19	-56.77	-56.91	-56.69
4	-57.95	-57.23	-57.61	-57.16
5	-58.13	-57.47	-55.77	-56.91
Delta	2.91	1.34	1.83	0.82
Rank	1	3	2	4
Optimum level	1	1	5	1

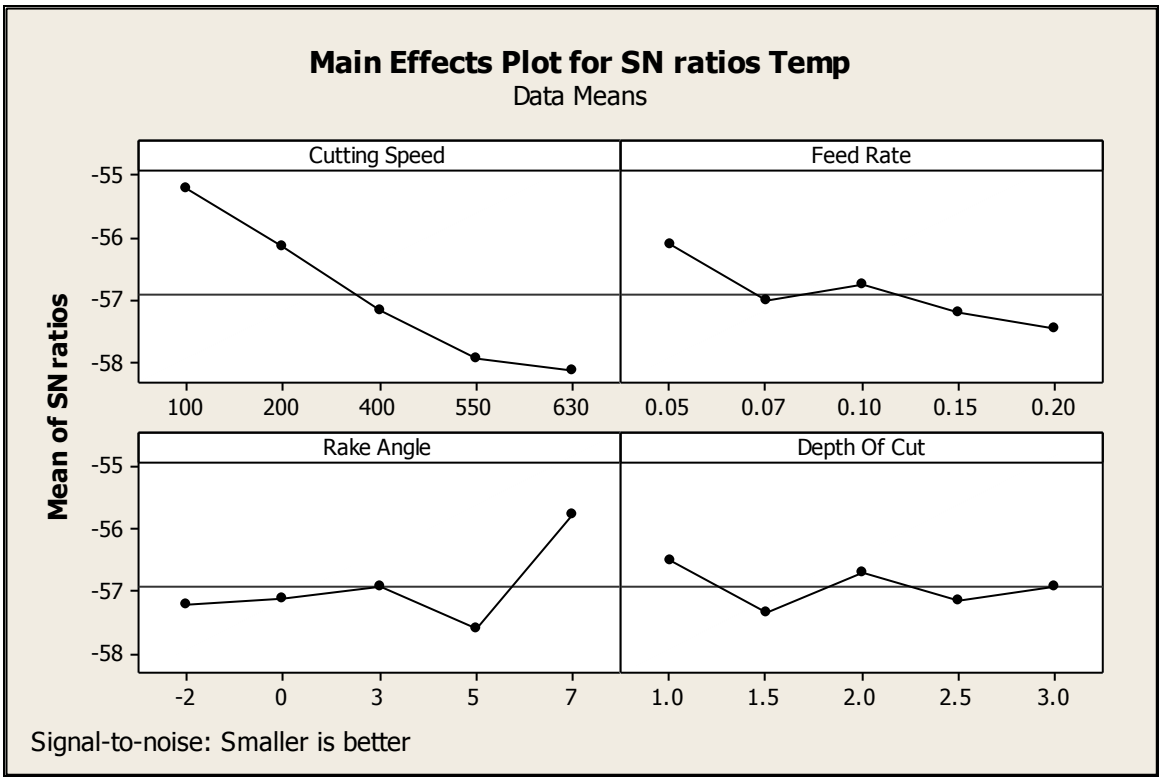

Figure 14 Plot for Main Effects for SN Ratios on Temp using Uncoated Cemented Carbide cutting tool (Source: Minitab®)

Table 16 and Figure 14 represent the response data for SN values of Temperature for Uncoated cemented Carbide cutting tool. As with the previous tool, it is observed here that for optimizing the temperature, the cutting speed has the most impact on outcomes followed by Rake Angle. The optimum values for these two factors are found to be same as previous tool i.e. 100 m/min and 7^{o}.

6.4.3 ANOVA:

ANOVA is used to analyze the experimental results and identifying the factors which have a significant effect on the machining output variables i.e. F_c and Temp. As explained in section 6.1.5 the SN ratio requires that the results be confirmed by ANOVA. The results of ANOVA are shown in Tables below. The p values or probability values show the level of significance of each factor. Lower p values indicate that, according to ANOVA tests, the factor values have higher probability of falling within the ranges which impact the outcome of the experiment. This should give the lowest p values for the factors which response data for SN ratios (refer previous section) have identified as having most impact on the outcome. Other results include its degree of freedom (DoF) which is defined as k-1 [53] (where k is number of levels), treatment sum of squares (SSTR), treatment mean squares (MSTR) and F statistics value which are defined previously.

Residual error is calculated statistically and has no physical influence on the experiment. It is however part of the ANOVA F-statistics test [53]. The DoF for residual error is calculated as (total Dof) – (sum of all treatment Dof). In case of Table 17, it is 24 – (4+4+4+4) = 8. The SSTR or SSE (Sum of squared error in case of residual error) is calculated by Eq. 6.6

$$SSE = (n_1 - 1)s_1^2 + (n_2 - 1)s_2^2 + \ldots + (n_j - 1)s_j^2 \qquad \textbf{Eq. 6.6}$$

Where "j" denotes each individual factor, "$s^{2"}$ is the variance and "n" is the number of observations in the j^{th} factor.

Analysis of Variance or ANOVA was carried out using the same software which works on the equations given in previous chapter. Results for ANOVA are given in Table 17, Table 18, Table 19 and Table 20.

Table 17 ANOVA Table of F_c using SN data for Carbide cutting tool (Source: Minitab®)

Source	DoF	SSTR	MSTR	F statistic	P value
Cutting Speed	4	1.392	0.3481	0.79	0.564
Feed Rate	4	168.835	42.2087	95.64	0
Rake Angle	4	0.662	0.1655	0.38	0.82
Depth Of Cut	4	264.313	66.0782	149.72	0
Residual Error	8	3.531	0.4413		
Total	24	438.733			

Table 18 ANOVA Table of Temp using SN data for Carbide cutting tool (Source: Minitab®)

Source	DoF	SSTR	MSTR	F statistic	P value
Cutting Speed	4	43.654	10.9136	25.06	0
Feed Rate	4	7.088	1.7721	4.07	0.043
Rake Angle	4	10.854	2.7135	6.23	0.014
Depth Of Cut	4	2.29	0.5725	1.31	0.343
Residual Error	8	3.485	0.4356		
Total	24	67.372			

Table 19 ANOVA Table of F_c using SN data for Uncoated Cemented Carbide cutting tool (Source: Minitab®)

Source	DoF	SSTR	MSTR	F statistic	P value
Cutting Speed	4	0.027	0.0068	0.05	0.994
Feed Rate	4	162.067	40.5168	308.22	0
Rake Angle	4	1.425	0.3563	2.71	0.107
Depth Of Cut	4	278.09	69.5225	528.86	0
Residual Error	8	1.052	0.1315		
Total	24	442.661			

Table 20 ANOVA Table of Temp using SN data for Uncoated Cemented Carbide cutting tool (Source: Minitab®)

Source	DoF	SSTR	MSTR	F statistic	P value
Cutting Speed	4	30.47	7.6174	9.11	0.004
Feed Rate	4	5.294	1.3236	1.58	0.269
Rake Angle	4	9.56	2.3899	2.86	0.096
Depth Of Cut	4	2.221	0.5552	0.66	0.634
Residual Error	8	6.688	0.836		
Total	24	54.232			

As evident from all four ANOVA tables, the p values for Feed Rate and Depth of cut are lowest when Cutting Forces are taken as output while p values for Cutting speed and Rake angle are lowest when Temperature values are concerned. This supports the previous results obtained by SN ratios and proves that for optimum values of cutting forces, feed rate and depth of cut should be optimized while for optimum values of Temperature, cutting speed and rake angle need to be optimized.

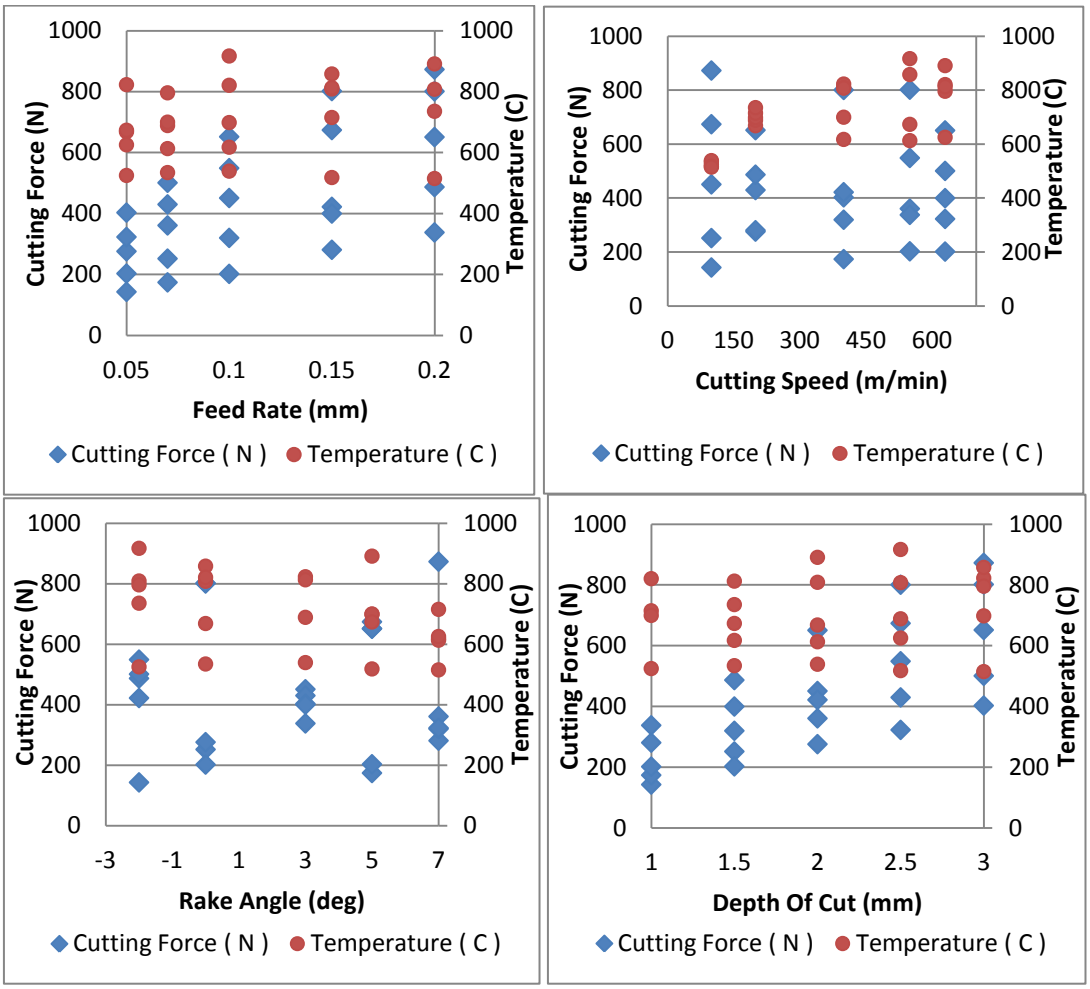

Figure 15 (a-d) Plots for F_c and Temp for all four factors for carbide cutting tool

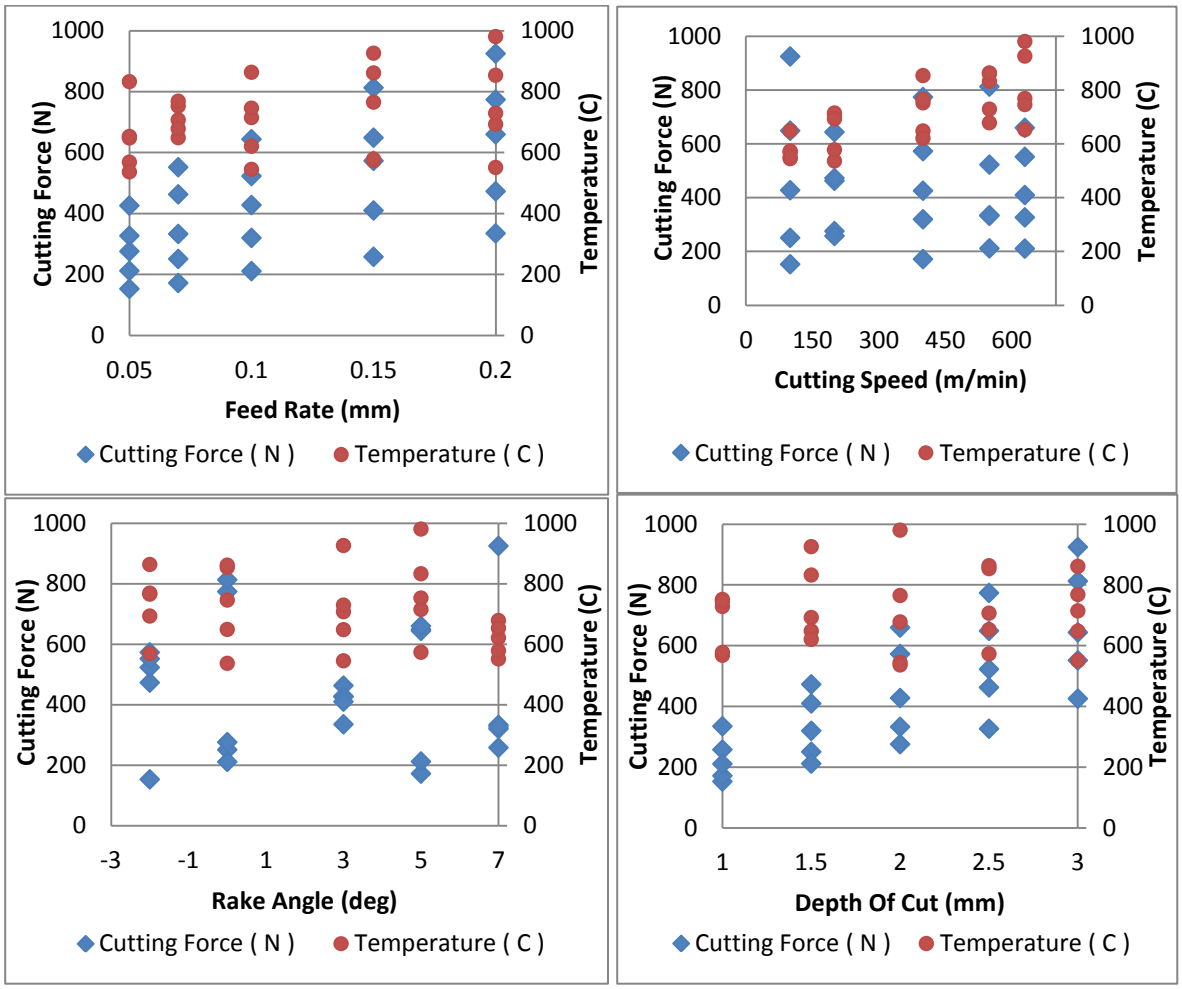

Figure 16 (a-d) Plots for F_c and Temp for all four factors for uncoated cemented carbide cutting tool

CHAPTER 7

CONFIRMATORY SIMULATIONS AND RESULTS

7.1 Optimum conditions for F_c:

As evident from the ANOVA p-values for F_c, the parameters which are most significant for optimization of cutting forces are Feed Rate and Depth of Cut with the other two factors having negligible effect.

With the help of response tables from S/N Ratio, the optimum levels for Feed Rate & Depth of Cut are found to be 0.05mm and 1mm respectively. The other two factors are also chosen according to the response tables but since their effect is considerably low, they are predictably different for both tools. Optimum levels of all parameters for minimum cutting force are given in Table 21.

Table 21 Optimum levels of input parameters for minimum Cutting Force

Parameter	Optimum Level for Carbide Cutting Tool	Optimum Level for Uncoated Cemented Carbide Cutting Tool
Cutting Speed (m/min)	400	100
Feed Rate (mm)	0.05	0.05
Rake Angle	-2	7
Depth Of Cut (mm)	1	1

The average for the treatment condition is predicted with the help of the means of all outputs for the experiments when they are performed at optimal levels. It is calculated in Eq. 7.1 [54]:

$$\eta_G = \bar{\eta}_G + (\bar{A}_o - \bar{\eta}_G) + (\bar{B}_o - \bar{\eta}_G) + (\bar{C}_o - \bar{\eta}_G) + (\bar{D}_o - \bar{\eta}_G) \quad \textbf{Eq. 7.1}$$

In Eq. 7.1 the term η_G is the S/N Ratio calculated at the optimum levels determined for minimum cutting force. $\bar{\eta}_G$ is the average of all S/N Ratios for F_c , $\bar{A}_o, \bar{B}_o, \bar{C}_o$ and $\bar{D}_o$ are the average S/N Ratios for cutting speed, feed rate, rake angle and depth of cut respectively when they are at optimum levels.

$$F_{cal} = 10^{\frac{-\eta_G}{20}} \quad \textbf{Eq. 7.2}$$

The cutting force output is calculated at optimum levels for both tools with the help of Eq. 7.2 and using η_G from Eq. 7.1. The calculated results are then verified using confirmatory experiments. These experiments are performed using the optimum levels of all 4 factors given in Table 21. Table 22 gives the results for predicted vs simulated outputs of cutting forces.

Table 22 Predicted vs Simulated Cutting Forces using optimum parameters

Tool	Predicted Cutting Force (N)	Simulated Cutting Force (N)	% error
Carbide Cutting Tool	130.2	136.4	4.46 %
Uncoated Cemented Carbide Cutting Tool	136.4	140	2.64%

7.2 Optimum conditions for Temperature:

According to the ANOVA p-values for temperature, the most important parameters for optimum levels of Temperature are Cutting Speed and Rake angle while the other two parameters are of little influence.

With the help of response table data from S/N Ratios, the optimum level of Cutting speed and Rake angle are found to be 100 m/min and 7^{o} respectively. Optimum levels of all parameters for minimum temperature are given in Table 23.

Table 23 Optimum levels of input parameters for minimum Temperature

Parameter	Optimum Level for Carbide Cutting Tool	Optimum Level for Uncoated Cemented Carbide Cutting Tool
Cutting Speed (m/min)	100	100
Feed Rate (mm)	0.05	0.05
Rake Angle	7	7
Depth Of Cut (mm)	1.5	1

$$T_{cal} = 10^{\frac{-\eta_G}{20}} \quad \textbf{Eq. 7.3}$$

Using Eq. 7.1 the S/N Ratio for optimum temperature is calculated by using temperature output data as input. Then with the help of Eq. 7.3, the temperature output at optimum levels for both tools is calculated. For verification, the calculated results are compared with confirmatory experiments performed using the optimum levels of all 4 factors given in Table 23. Table 24 gives the results for predicted vs simulated outputs of Temperature.

Table 24 Predicted vs Simulated Temperature values using optimum parameters

Tool	Calculated Temperature (^{o}C)	Simulated Temperature (^{o}C)	% error
Carbide Cutting Tool	406.4	396.3	2.48%
Uncoated Cemented Carbide Cutting Tool	439.5	424.2	3.47%

CHAPTER 8

DISCUSSION

Figure 15 and Figure 16 represent the variations in cutting speed and temperature for all four factors at different levels for carbide cutting tool and uncoated cemented carbide cutting tool respectively. From the graphs it can be observed that:

1. The cutting forces form an escalating trend with increasing feed rate and depth of cut in both tools. This is understandable as increasing feed and depth of cut will increase material removal rate independent of the tool as explained in chapter 2.3 and increase in MRR will always require more forces.
2. As the feed rate and depth of cut is reduced, the cutting forces seem to converge which shows stability and less dependence on other factors. This is evident from SNR and ANOVA as they show that the optimum levels for both these factors is the lowest level since it has the least variance.
3. While Feed Rate and Depth of Cut do not seem to follow a specific trend in case of Temperature values, the cutting speed is observed to respond better when Temperature values are concerned. Although cutting speed is a factor of the MRR as shown in Eq. 2.1, it is directly responsible for generating frictional values and hence increasing cutting speed will result in increasing temperature.
4. Temperature converges to lower values when cutting speed is low. This is due to the fact that less speed generates less friction and as a consequence, less heat is generated.
5. Rake angle, as shown in Figure 15 and Figure 16, is the most irregular of all factors and it seems to barely relate with cutting forces. However, as it is increased, a converging trend is observed in temperature and hence minimum variance in temperature is observed with highest Rake angle values. As the rake angle goes higher, the motion of chip is less perpendicular to the relative motion of tool and workpiece hence there will be less work done against the motion causing lesser friction. This would amount to a decrease in temperature.

Table 22 and Table 24 show the results of confirmatory simulations in which the optimum values for all four parameters were used as input and cutting forces and temperatures were taken as output.

CHAPTER 9

CONCLUSIONS

It is found that:

1. The carbide cutting tool is a better option while machining AISI 1045 steel as it results in lower cutting forces and temperature values as compared to uncoated cemented carbide cutting tool.
2. The most significant factors for cutting forces are feed rate and depth of cut with minimum possible p-values of 0 for both tools. Similarly, the most significant factors for temperature is cutting speed with p-values of 0 and 0.004 for both tools. At a confidence level of 95%, these values fall well under the criteria to be deemed as significant factors.
3. For the carbide cutting tool, the rake angle is observed to be significant for lower temperatures as its p-value of 0.014 is within the range of 95% confidence level but for uncoated carbide cutting tool, rake angle is not found to be significant factor in lowering the temperature as its p-value is at 0.096.
4. The optimum values of cutting force and temperature as calculated statistically is well within 5% error range of the simulated results which shows that the analysis results obtained were satisfactory as the output is optimized by using optimized parameters. ANOVA has reinforced the results of SN ratio by statistically proving the probability factors to be within 5% confidence level.
5. The optimum machining conditions when machining AISI 1045 steel using a carbide cutting tool, are given in Table 23

Orthogonal cutting process of AISI 1045 Steel has been modeled successfully in this study using general purpose code ABAQUS® and the model was validated by experimental results reported in literature. For simplicity a two-dimensional model was used and the tool was assumed to be rigid. Furthermore, the coefficient of friction was taken to be constant based on literature values.

Four parameters of orthogonal cutting namely Cutting Speed, Feed Rate, Rake Angle and Depth of Cut were to be optimized and Taguchi matrix was used for designing the experiment using two different type of carbide cutting tools. The influence of these parameters on the machining outputs of AISI 1045 Steel has been studied in order to optimize the parameters to provide lower cutting forces and temperature values. A total of 25 simulations were run with each tool using five levels of each of the four input parameters.

The responses from the experiments were subjected to statistical analysis using the multipurpose software Minitab® V16 and optimum levels of each parameter for both tools were determined. Minimized values for cutting forces and temperatures for each tool using optimized factors were predicted and verified using confirmatory simulations.

CHAPTER 10

AREAS OF FUTURE WORK

Orthogonal cutting, while being a primitive subject and one of the most commonly and easily used tool for metal cutting, is still a very vast field and quite a lot can be researched and streamlined in this subject. Related to the current work, it is recommended that work be carried out to minimize the forces of friction and stresses in orthogonal cutting along with optimizing more input factors using advanced simulations.

A wide variety of tools and workpieces are worked upon in this era which gives a huge window of opportunity for future researchers and lots of flexibility in choosing their materials.

With regards to the types of simulation, research should be done in 3D simulations which will help get more detailed and in depth analysis of the process.

REFERENCES

[1]. M. Nalbant, H. Go¨Kkaya, G. Sur. Application Of Taguchi Method In The Optimization Of Cutting Parameters For Surface Roughness In Turning. 2006.

[2]. http://www.tatasteelnz.com/downloads/meduimtens_aisi1045.pdf

[3] Mahmoud Al Bawaneh: Determination Of Material Constitutive Models Using Orthogonal Machining Tests; Published In 2007 By Wichita State University, College Of Engineering, Department Of Industrial And Manufacturing Engineering (2007)

[4] Ozel T. And E. Zeren: "A Methodology To Determine Work Material Flow Stress And Tool Chip Interfacial Friction Properties By Using Analysis Of Machining"; Journal Of Manufacturing Science And Engineering, Vol 128 (2006) 119-129 DOI: 10.1115/1.2118767

[5] Sartkulvanich P., F. Koppka And T. Altan: Determination Of Flow Stress For Metal Cutting Simulation – A Progress Report; Journal Of Material Processing Technology, Vol 146, (2004) Pp 61-71

[6] E. Ceretti, P. Fallbohmer, W. T. Wu C, T. Altan: Application Of 2d Fem To Chip Formation In Orthogonal Cutting; J. Mater. Process. Technol. 59 (1996) 169-180

[7] M.P. Groover, "Fundamentals of Modern Manufacturing 2ed". John Wiley and Sons, Inc. 2002 ©

[8] M.E. Merchant, Mechanics of the Metal Cutting Process, J. Appl. Physics, Vol 16 (No. 6), 1945, p 318-324

[9] E.H. Lee and B.W. Schaffer, Theory of Plasticity Applied problems of Machining, ASME J. Appl. Mech., Vol 18 (No. 4), 1951, p 104-113

[10] A.O. Tay, M.G. Stevenson, and G. De Vahl Davis, Using the Finite Element Method to Determine Temperature Distributions in Orthogonal Machining, Proc Inst. Mech. Eng., Vol 188, 1974, p 627-637

[11] J.C. Lemaire And W.A. Backofen: Adiabatic Instability In The Orthogonal Cutting Of Steel; Metallurgical Transactions Volume 3, Feb 1972

[12] G. Caprino, I.De Lorio, L. Nele, And L. Santo: Effect Of Tool Wear On Cutting Forces In The Orthogonal Cutting Of Unidirectional Glass Fibre-Reinforced Plastics; Composites Part A 27-A Elsevier Science Limited (1996) 409-415

[13] J.Wang, C.Z Huang, W.G Song: The Effect Of Tool Flank Wear On The Orthogonal Cutting Process And Its Practical Implications; Journal Of Materials Processing Technology 142 (2003) 338- 346

[14] G. Boothroyd, Photographic technique for the determination of metal cutting temperatures, British J. Appl. Phys. 12 (1961) 238–242

[15] M.C. Shaw, Some observations concerning the mechanics of cutting and grinding, Appl. Mech. Rev. 46 (1993) 74–79.

[16] M.E. Merchant, Basic mechanics of the metal cutting process, J. Appl. Mech. 11 (1944) A168–A175

[17] V. Piispanen, Theory of formation of metal chips, J. Appl. Phys. 19 (1948) 876–881

[18] P.L.B. Oxley, Shear angle solutions in orthogonal machining, Int. J. Mach. Tool Des. Res. 2 (1962) 219–229.

[19] E.H. Lee, B.W. Shaffer, The theory of plasticity applied to a problem of machining, J. Appl. Mech. 18 (1951) 405–413.

[20] H. Kudo, Some new slip-line solutions for two-dimensional steady-state machining, Int. J. Mech. Sci. 7 (1965) 43–55.

[21] W.B. Palmer, P.L.B. Oxley, Mechanics of orthogonal machining, Proc. Inst. Mech. Eng. 173 (1959) 623–638.

[22] P.L.B. Oxley, A.G. Humphreys, A. Larizadeh, The inGuence of rate of strain-hardening in machining, Proc. Inst. Mech. Eng. 175 (1961) 881–891

[23] E.D. Doyle, J.G. Horne, D. Tabor, Frictional interactions between chip and rake face in continuous chip formation, Proc. Roy. Soc. Land. A 366 (1979) 173–183.

[24] W.B. Heginbotham, S.L. Gogia, Metal cutting and the built-up nose, Proc. Inst. Mech. Eng. 175 (1961) 892–917

[25] K. Komvopoulos and S.A. Erpenbeck, Finite Element Modeling of Orthogonal Metal Cutting, J. Eng. Industry, Vol 113, 1991, p 253-267

[26] B. Zhang and A. Bagchi, Finite Element Simulation of Chip Formation and Comparison with Machining Experiment, Computational Methods in Materials Processing, PED-Vol. 61, ASME, 1992, p 61-74

[27] G.S. Sekhon and J.L. Chenot, Numerical Simulation of Continuous Chip Formation During Non-Steady Orthogonal Cutting, Eng. Comp., Vol 10, 1993, p 31-48

[28] E.G. Ng, D.K. Aspinwall, D. Brazil, and J. Monagham, Modelling of Temperature and Forces when Orthogonally Machining Hardened Steel, Int. J. Mach. Tools Manuf., Vol 39, 1999, p 885-903

[29] A.G. Mamalis, M. Horvath, A.S. Branis, and D.E. Manolakos, Finite Element Simulation of chip Formation in Orthogonal Metal Cutting, J. Mater. Proc. Technol., Vol 110, 2001, p 19-27

[30] M.H. Dirikolu, T.H.C. Childs, and K. Maekawa, Finite Element Simulation of Chip Flow in Metal Machining, Inter. J. Mech. Sci., Vol 43, 2001, p 2699-2713

[31] Patricia Muñoz-Escalona, Shreyes Melkote, And Kai Liu: Influence Of The Stress, Strain, And Temperature On The Surface Roughness Of An Aisi 52100 Steel Due To An Orthogonal Cut; Journal Of Materials Engineering And Performance Jmepeg (2005) 14:582-590

[32] Mang Sung Choi: A Study Of Shear Angle Relationships In Shearing Process On The Shear Plane And The Rake Face In Orthogonal Cutting; Ksme Journal, Vol 9, No.3 (1994) 385 – 391

[33] Linhu Tang, Jianlong Huang , Liming Xie: Finite Element Modeling And Simulation In Dry Hard Orthogonal Cutting Aisi D2 Tool Steel With Cbn Cutting Tool; International Journal Of Advanced Manufacturing Technology (2011) 53:1167–1181

[34] Xiaomin Deng, Chandrakanth Shet: Finite Element Analysis Of The Orthogonal Metal Cutting Process; Journal Of Materials Processing Technology 105 (2000) 95-109

[35] M. Movahhedy, M.S. Gadala*, Y. Altintas: Simulation Of The Orthogonal Metal Cutting Process Using An Arbitrary Lagrangian Eulerian Finite-Element Method; Journal Of Materials Processing Technology 103 (2000) 267-275

[36] Guoqin Shi, Xiaomin Deng, Chandrakanth Shet: A Finite Element Study Of The Effect Of Friction In Orthogonal Metal Cutting; Finite Elements In Analysis And Design 38 (2002) 863–883

[37] K. Li, X.-L. Gao, J.W. Sutherland: Finite Element Simulation Of The Orthogonal Metal Cutting Process For Qualitative Understanding Of The Effects Of Crater Wear On The Chip Formation Process; Journal Of Materials Processing Technology 127 (2002) 309-324. doi:10.1016/S0924-0136 (02)00281-9

[38] C. Shet, X. Deng: Residual Stresses And Strains In Orthogonal Metal Cutting; International Journal Of Machine Tools & Manufacture 43 (2003) 573–587

[39] Faraz Akbar & Paul T. Mativenga & M. A. Sheikh: An Experimental And Coupled Thermo-Mechanical Finite Element Study Of Heat Partition Effects In Machining Int J Adv Manuf Technol (2010) 46:491–507 doi:10.1016/0013-7944 (85)90052-9

[40] M. Mohammadpour, M.R. Razfar *, R. Jalili Saffar: Numerical Investigating The Effect Of Machining Parameters On Residual Stresses In Orthogonal Cutting; Simulation Modelling Practice And Theory 18 (2010) 378–389

[41] K. Komvopoulos, S.A. Erpenbeck, Finite element modeling of orthogonal metal cutting, J. Eng. Ind. 113 (1991) 253–267.

[42] T. Tyan, W.H. Yang, Analysis of orthogonal metal cutting processes, Int. J. Num. Meth. Eng. 34 (1992) 365–389.

[43] Aviral Shrot, Martin Bäker: Is It Possible To Identify Johnson-Cook Law Parameters From Machining Simulations? ; Technische Universität Braunschweig, Institut für Werkstoffe, Germany Int J Mater Form (2010) Vol. 3 443– 446

[44] Johnson G.R., Cook W. H. : Fracture Characteristics Of Three Metals Subjected To Various Strains, Strain Rates, Temperatures And Pressures. Eng Fract Mech 21(1): 31-48 (1985)

[45] O. Pantale, J.-L. Bacaria, O. Dalverny, R. Rakotomalala, S. Caperaa: 2D And 3D Numerical Models Of Metal Cutting With Damage Effects; Comput. Methods Appl. Mech. Engrg. 193 (2004) 4383–4399 Doi:10.1016/J.Cma.2003.12.062

[46] Mabrouki T, Rigal J-F: A Contribution To A Qualitative Understanding Of Thermo-Mechanical Effects During Chip Formation In Hard Turning; J Mater Process Technol (2006) 176:214–221. Doi:10.1016/J.Jmatprotec.2006.03.159

[47] Guo YB, Yen DW: A FEM Study On Mechanisms Of Discontinuous Chip Formation In Hard Machining; J Mater Process Technol (2004) 155–156:1350–1356. Doi:10.1016/J.Jmatprotec.2004.04.210

[48] J. Lorentzon, N. Jarvstrat: modeling tool wear in cemented carbide machining alloy 718; International journal of Machine Tools & Manufacture 48 (2008) 1072-1080

[49] ALE Adaptive Meshing: Overview Chapter 12.2.1 Abaqus Analysis User's Manual Abaqus Documentation 6.10

[50] http://www.ecs.umass.edu/mie/labs/mda/fea/sankar/chap2.html\

[51] Fundamentals of Quality Control and Improvement by Amitava Mitra 2nd Edition pages 552-556 and 595-625

[52] Robert L. Mason; Statistical Design and Analysis of Experiments With Applications to Engineering and Science Second Ed. Copyright 2003 by John Wiley and Sons, Inc.

[53] Neil A Weiss: Introductory Statistics 9th Ed. School of Mathematical and Statistical Sciences Arizona State University ISBN-13: 978-0-321-69122-4

[54] Emre Yu Cel And Mustafa Gunay: Modelling And Optimization Of The Cutting Conditions In Hard Turning Of High-Alloy White Cast Iron (Ni-Hard) Proceedings Of The Institution Of Mechanical Engineers, Part C: Journal Of Mechanical Engineering Science Published Online 20 December 2012 DOI: 10.1177/0954406212471755

[55] İrfan Ucun & Kubilay Aslantas: Numerical simulation of orthogonal machining process using multilayer and single-layer coated tools; Int J Adv Manuf Technol (2011) 54:899–910 DOI 10.1007/s00170-010-3012-9

[56] Gary W. Oehlert, University of Minnesota (2010). A First Course in Design and Analysis of Experiments. ISBN 0-7167-3510-5 Copyright © 2010 Gary W. Oehlert

[57] Stephanie Fraley, Mike Oom, Ben Terrien and John Zalewski; Design of experiments via taguchi methods: orthogonal arrays.
https://controls.engin.umich.edu/wiki/index.php/Design_of_experiments_via_taguchi_methods:_orthogonal_arrays Date Presented: 12/5/06; Revised: 11/27/07